*ISSN: 2357-0547 (Print)*
*ISSN: 2357-0539 (Online)*

*Research Article / JAPR / Sec. B*
*Akinwumi et al., 2023, 7 (4),* **205-231**

**Journal of Advanced Pharmacy Research**

**Section B: Pharmaceutical Analytical & Organic Chemistry, Medicinal & Biochemistry**

# Therapeutic Potential and Molecular Docking Perspective of Six Medicinal Plants Against the Human SIRT-6 Protein Implicated in Type-2 Diabetes

Ishola A. Akinwumi[1]*, Barakat O. Ishola [2], Riswat F. Musbau[3], Aishat E. Abubakar[4], Adefolarin P. Owojuyigbe[5]

[1]*Department of Chemistry, Faculty of Chemistry and Chemical Technology, University of Ljubljana, Ljubljana, Slovenia.* [2]*Department of Biomedical Technology, School of Basic Medical Sciences, Federal University of Technology, Akure, Ondo State, Nigeria.* [3]*Department of Pharmaceutical Chemistry, Faculty of Pharmacy, University of Lagos, Lagos Nigeria.* [4]*Department of Biochemistry, Faculty of Science Laboratory Technology, Federal Polytechnic Ilaro, Ogun State Nigeria* [5]*Department of Chemistry, School of Physical Sciences, Federal University of Technology, Akure, Ondo State, Nigeria.*

***Corresponding author:** Ishola A. Akinwumi, Department of Chemistry, Faculty of Chemistry and Chemical Technology, University of Ljubljana, Ljubljana, Slovenia. Tel. + +38669660471*

*Email address: akinwumiishola5000@gmail.com*

***Submitted on: 12-07-2023; Revised on: 19-08-2023; Accepted on: 19-08-2023***

**To cite this article:** Akinwumi, I. A.; Ishola, B. O.; Musbau, R. F.; Abubakar., A. E, Owojuyigbe, A. P. Therapeutic Potential and Molecular Docking Perspective of Six Medicinal Plants Against the Human SIRT-6 Protein Implicated in Type-2 Diabetes. *J. Adv. Pharm. Res.* **2023**, *7* (4), 205-231. DOI: 10.21608/aprh.2023.222618.1226

## ABSTRACT

**Objective:** Despite the vast array of approved anti-diabetic drugs and the fact that these medications are often associated with other serious side effects like cardiovascular disease, weight gain, liver disorders, and countless others, the prevalence of Type-2 diabetes is soaring. Through *in silico* analysis, our study seeks to elucidate the anti-diabetic potential of six (6) medicinal plants *Buchholzia coriacea*, *Vernonia amygdalina*, *Mimosa pudica*, *Momordica charantia*, *Bergenia ciliate*, and *Mangifera indica*. **Methods**: Twenty-nine (29) bioactive compounds were selected from the six plants. Metformin and Miglitol are used as the control drug in this study. PubChem, an online server, was used to get the 3D structure of the bioactive compounds and the control drugs. The protein data bank was used to retrieve the crystal structure of the SIRT6 protein. The SwissADME online server was used for the Drug-likeness of the bioactive compounds and the control drugs. AutoDock was used for the molecular docking of compounds that passed the drug-likeness with the SIRT6 active site. The protein-ligand complexes were analyzed using a protein-ligand interaction profiler and proteins plus web server. The Molinspiration online server was used to predict compound bioactivity. The ADMETlab webserver was used to determine the ligands' ADMET properties. **Results:** The drug-likeness screening of the twenty-nine compounds and the control drugs revealed that twenty-five compounds have zero or one violation of Lipinski's rule of five. Metformin and Miglitol have zero violations. The docking analysis revealed that twenty out of the twenty-five compounds docked against the protein target have better binding affinity than the control drugs. Catechin, Luteolin, Chlorogenic acid, and Mimopudine have an excellent binding affinity of -8.4 kcal/mol -7.8 kcal/mol, -7.7 kcal/mol, and -7.5 kcal/mol, respectively. In contrast, Metformin and Miglitol have binding scores of -4.8 and -5.1 kcal/mol, respectively. **Conclusions:** Therefore, the greater binding affinity of the twenty compounds compared to the control drugs suggests that these compounds possess anti-diabetic properties with good interaction with the SIRT6 protein. However, this research needs further validation with molecular dynamics studies and *in-vitro* and *in-vivo* evaluation.

***Keywords:*** *Molecular docking, Anti-diabetic, Type-2 diabetes, Drug-likeness, Molecular dynamics.*

## INTRODUCTION

Diabetes mellitus (DM), commonly called diabetes, encompasses a collection of metabolic disorders characterized by elevated blood sugar levels[1]. Insulin and glucagon play crucial roles in regulating the average glucose levels in the body. Insufficient insulin production, resistance to insulin action, or a combination of both often leads to impaired metabolism of carbohydrates and lipids, resulting in increased fasting and post-meal blood sugar levels[2]. If left untreated, persistently high blood sugar levels associated with diabetes can cause damage to various organs, such as nerves, eyes, and kidneys, and even be fatal. Long-term complications of diabetes include diabetic retinopathy (vision loss), diabetic nephropathy, peripheral/autonomic neuropathy, and cardiovascular diseases[3].

Furthermore, individuals with diabetes are more prone to developing atherosclerosis and cerebrovascular diseases[4]. The statistics surrounding diabetes are concerning, despite the existence of standard anti-diabetic medications. According to the World Health Organization (WHO), the global prevalence of diabetes among individuals aged 20 to 79 was estimated to be 8.8% in 2015 and is projected to rise to 10.4% by 2040[5]. The international diabetes federation predicts that by 2040, 642 million individuals will have been diagnosed with diabetes[6]. The most prevalent forms of diabetes include Type 1 Diabetes (Insulin Dependent), Type 2 Diabetes (Non-Insulin Dependent), and Gestational Diabetes[7]. Type 2 diabetes arises when there is a significant impairment in insulin action, known as insulin resistance (IR), resulting in cellular dysfunction due to the pancreatic β-cells' inability to compensate for IR. Insulin resistance refers to the compromised ability of muscle, liver, and adipose tissue to appropriately respond to insulin's metabolic effects[8]. It accounts for approximately 90% of all diabetes cases and contributes to global morbidity and mortality. Consequently, there is a demand for new and effective treatments that can enhance metabolic control and reduce the incidence of complications[9]. Existing treatments encompass various approaches such as stimulating increased insulin secretion from the pancreas (e.g., Sulfonylureas like Glibenclamide, Glipizide, Chlorpropamide, Tolbutamide, and Glimepiride), enhancing target organ sensitivity to insulin (e.g., Thiazolidinediones like Rosiglitazone and Pioglitazone), and slowing down glucose absorption from the gastrointestinal tract (e.g., alpha-glucosidase inhibitors like Acarbose and Miglitol) [10]. However, these antidiabetic therapies are associated with adverse effects such as liver disorders, cardiovascular diseases, weight gain, bloating, flatulence, diarrhoea, and abdominal discomfort[11].

Sirtuin-6 (SIRT6) belongs to the Sirtuin family and regulates various physiological processes, including intermediary metabolism, ageing, genomic stability, and tumorigenesis[12]. In terms of glucose metabolism, targeting SIRT6 presents an attractive opportunity for the development of novel and effective antidiabetic treatments, as evidenced by animal studies showing enhanced expression of glucose transporters, increased tissue glucose uptake, and reduced blood glucose levels in Sirt6-deficient mice[9]. The impact of SIRT6 on glucose metabolism primarily stems from its ability to repress the transcription factor hypoxia-inducible factor-1α epigenetically (HIF1-α) [13]. Consequently, the deletion of SIRT6 leads to elevated HIF1-α-mediated transcription, resulting in increased expression of glucose transporters and glycolytic enzymes. Therefore, compounds that inhibit SIRT6 have the potential to be valuable antidiabetic agents by enhancing glucose uptake and promoting glycolysis. Notably, SIRT6 has also been shown to regulate gluconeogenesis by modulating the activity of peroxisome proliferator-activated receptor-γ coactivator 1α, suppressing hepatic glucose production[14]. Based on this effect, exploiting the activation of SIRT6 has been proposed as a strategy for antidiabetic treatment[15]. Since diabetes is a complex disease involving multiple factors, targeting multiple pathways holds more promise than a single-focused therapeutic approach in effectively managing diabetes. The limitations and adverse effects associated with currently available antidiabetic agents, whether in terms of effectiveness or safety, have prompted the search for novel drugs that can more efficiently manage type II diabetes. Approximately 60% of the global population depends on traditional remedies for addressing diverse ailments[16], and numerous medicinal plants have been traditionally employed for managing diabetes. Over 400 plant species have been documented for their potential in diabetes treatment. Nevertheless, only a limited number of these plants have undergone rigorous scientific evaluation, and the underlying mechanisms by which these plants exert their medicinal effects still need to be discovered[16].

*Momordica charantia*, commonly known as bitter melon, belongs to the *Cucurbitaceae* family and is extensively cultivated in numerous tropical and subtropical regions worldwide[17]. It encompasses diverse distinct and biologically active phytochemicals, such as Triterpenes, Steroids, Glycosides, Saponins, and Alkaloids[18]. Extracts derived from various parts of this plant have been reported to exhibit hypoglycemic properties[19, 20]. The hypoglycemic effects of *Momordica charantia* fruit juice have been observed in animal models of experimental diabetes and individuals with both type-1 and type-2 diabetes mellitus[21].

*Bergenia ciliata*, referred to as "Pashanbheda" in Nepalese communities, has a long-standing traditional

use in treating diabetes independently or in combination with other therapies[22]. The rhizome of *Bergenia ciliata* is rich in Bergenin, a prominent glycoside, and contains a novel lactone called paashanolactone[23]. Additionally, the aerial parts of this plant contain Bergenin alongside other Glycosides and Flavonoids[24]. Numerous secondary metabolites present in *B. ciliata*, including Catechin, Gallicin, Gallic acid, β-sitosterol, Bergenin, and Tannic acid, contribute to its biological activities, which encompass antibacterial, anti-inflammatory, antitussive, antiulcer, and anti-diabetic properties[25- 29].

*Mimosa pudica*, known locally as "Lajjawati," contains a rich assortment of valuable phytochemicals[30] such as Mimosine, Stigmasterol, β-sitosterol, Betulinic acid, *p*-coumaric acid, Mimopudine, 2-Hydroxymethylchroman-4-one, Quercetin, and Avicularin. These phytochemicals are associated with various pharmacological properties, including antibacterial, antivenom, wound healing, anti-cancer, and antidiabetic effects[31-33]. Many of these phytochemicals, or derivatives obtained through chemical modification of plant compounds, have been utilized to enhance the safety of pharmaceutical drugs.

*Buchholzia coriacea* is a perennial plant from the Capparaceae family, known for its medicinal potential and often used in herbal medicine. The plant grows as a forest tree, and its seeds, referred to as "good kola," are widely consumed and can be cooked or eaten raw[34]. In Africa, it is recognized for its beneficial properties in treating hypertension, preventing premature ageing, and enhancing memory function. Additionally, the bark decoction is utilized for washing individuals with smallpox. At the same time, the young leaves are applied as a poultice for boils, and the seeds serve as condiments or cough medicine[35, 36].

*Vernonia amygdalina*, commonly known as 'Bitter leaf', belongs to the Asteraceae family[37]. It is a shrub that reaches a height of 2 to 5 meters and possesses a significant amount of bitter compounds throughout its various parts[38] In Nigeria, this local plant is widely utilized for both therapeutic and nutritional purposes and is a crucial ingredient in the production of 'bitter leaf soap'[39]. The cultivation of *Vernonia amygdalina* in Nigeria primarily focuses on its nutritional value[39]. The fresh leaf extract of this plant has been found to contain a range of compounds such as Alkaloids, Saponins, Tannins, Flavonoids, Anthraquinones, Glycosides, Terpenoids, Proteins, Vitamins, and Minerals[40, 41].

*Mangifera indica*, belonging to the Anacardiaceae family, is a large evergreen tree known for its dense foliage and substantial size, reaching heights of 10 to 45 meters[42]. It has a sturdy trunk from which heavily branched branches emerge[43]. Traditional medicine has utilized extracts from *Mangifera indica* to treat various ailments, including diabetes, bronchitis, diarrhoea, asthma, renal disorders, scabies, respiratory issues, syphilis, and urinary diseases[44, 45]. The biologically active component of *Mangifera indica* is Mangiferin, which is followed by Benzophenones, Phenolic acids, and other antioxidants such as Flavonoids, Carotenoids, Quercetin, Isoquercetin, Ascorbic acid, and Tocopherols. These phytochemicals found in *Mangifera indica* exhibit a range of pharmacological properties, including antioxidant, anti-diabetic, anti-inflammatory, antimicrobial, antiviral, immunomodulatory, anti-obesity, anti-allergic, antifungal, antiparasitic, antidiarrheal, antipyretic, and anti-tumour activities[45].

*Molecular docking* is a simulation strategy that relies on the structural characteristics of proteins and ligands to predict their interactions. This technique utilizes a scoring system to evaluate the affinity of the interaction and identifies the binding site on the target receptor[46]. Based on this knowledge, we have conducted an *in silico* comparison to assess the potential of natural compounds, including *Momordica charantia*, *Buchholzia coriacea*, *Vernonia amygdalina*, *Mimosa pudica*, *Bergenia ciliate*, and *Mangifera indica*, in comparison to commonly used conventional drugs (Metformin and Miglitol) as antidiabetic agents. We have also performed *in silico* predictions to evaluate these compounds' drug-likeness, bioactivity, absorption, distribution, metabolism, excretion, and toxicity (ADMET) properties.

## MATERIAL AND METHODS

### Selection of Ligands (Bioactive compounds)

In this study, six (6) medicinal plants were selected, namely *Buchholzia coriacea* (Wonderful Kola), *Vernonia amygdalina* (Bitter Leaf), *Mimosa pudica* (Sleepy Plant), *Momordica charantia* (Bitter Melon), *Bergenia ciliate* (Fringed Bergenia), and *Mangifera indica* (Mango) [47-53]. Twenty-nine (29) bioactive compounds were selected from the six (6) plants. Additionally, control drugs used in the study included Metformin and Miglitol. Table 1 presents the bioactive compounds selected from the plants and the control drugs. To obtain the PubChem identification number (PID), the 3D structure in Structural Data Format (SDF), and the canonical SMILES of the bioactive compounds and control drugs, we used a chemical repository server called PubChem Web (https://pubchem.ncbi.nlm.nih.gov/) [54].

### Selection of Protein Target

The protein of interest in this study is human SIRT6, and its crystal structure was obtained from the literature[55]. The three-dimensional (3D) crystallographic structure of the target protein (PDB: 3K35) [55] was acquired from the Research Collaboratory of Structural Bioinformatics (RCSB) Protein Database

(https://www.rcsb.org/ ) [56] and saved in the PDB format. **Figure 2** illustrates the structure of the human SIRT6 protein crystal.

**Preparation of Protein Target**

The human SIRT6 crystal structure underwent cleaning and preparation, involving the removal of co-crystallized ligands using UCSF Chimera (version 1.13.1)[57]. UCSF Chimera was utilized to eliminate water molecules, introduce hydrogen atoms, and assign Gasteiger-Huckel charges. The protein was then subjected to minimization for molecular docking purposes and saved in PDB format.

**Screening for Drug-likeness**

The bioactive compounds and the control drugs were subjected to drug-likeness screening using the online server SwissADME (http://swissadme.ch/)[58]. This screening utilized the canonical SMILES of the compounds. Out of the twenty-nine (29) bioactive compounds and two (2) control drugs, four (4) bioactive compounds violated multiple criteria of the Lipinski rule of five[59]. The remaining compounds were then subjected to molecular docking.

**Molecular docking**

The software PyRx[60] was employed to conduct molecular docking between the ligands and the target protein. The downloaded 3D structures of the ligands were sequentially uploaded to PyRx, where they were optimized to their lowest energy state using the Merck molecular force field (MMFF94). Subsequently, the ligands were converted to the auto-dock ligand format (PDBQT). The AutoDock was utilized to perform the molecular docking study, utilizing a lattice box with mean dimensions (x: 41.4429, y: 14.8822, z: 53.6957) and sizes (x: 62.7600, y: 93.2744, z: 56.8412 angstroms) to define the active site of the protein. A selection of amino acids identified from the literature, and known to be present in the binding region of the target protein, was used for molecular docking[55, 61]. The resulting binding energy in kcal/mol was obtained for each ligand and the protein complex. Additionally, PyRx was used to convert the docked ligands and protein targets from the PDBQT format to the PDB format, allowing for further analysis and visualization of the results.

**Analysis of Molecular Interactions**

The protein-ligand complexes were analyzed using PyMOL molecule visualization software (version 2.4, 2010, Schrödinger LLC) [62] to generate graphical representations. The resulting complexes were saved in PDB format. Subsequently, these complexes were uploaded to the web servers Protein-Ligand Interaction Profiler (https://plip-tool.biotec.tu-dresden.de/plip-web/plip/index) [63] and Proteins Plus (https://proteins.plus/) [64, 65] to identify and analyze their molecular interactions.

**Bioactivity Prediction**

The bioactivity of the ligands was assessed utilizing the online server Molinspiration (https://www.molinspiration.com) [66]. This server calculated the activity score for various categories, including GPCR ligands, ion channel modulators, nuclear receptor ligands, kinases, proteases, and enzyme inhibitors. A specific range was utilized to determine the organic compounds' bioactivity. A compound is classified as active if its bioactivity score exceeds 0 (>0). The compound is moderately active if the score falls between -5.0 and 0.0. On the other hand, if the score is less than -5.0 (<-5.0), the compound is regarded as inactive [66].

**ADMET Properties prediction**

The pharmacokinetic properties of the ligands were evaluated using the online tool ADMETlab (https://admetmesh.scbdd.com/service/evaluation/cal) [67]. This tool allowed for assessing the absorption, distribution, metabolism, excretion, and toxicity (ADMET) properties of the ligands derived from the molecular docking process. The obtained results were then utilized to predict the pharmacokinetic properties of the ligands.

## RESULTS

**Drug-Likeness Screening Of Selected Compounds**

The bioactive compounds selected from the six medicinal plants were subjected to drug-likeness screening using the SwissADME server. The screening process involved applying the Lipinski rule of five. Among the compounds, twenty-five (25) exhibited no more than one violation of the Lipinski rule of five and were consequently considered for further analysis in this research. However, four (4) compounds violated two rules and were excluded from further analysis. As for the control drugs used in the study, Metformin and Miglitol, they did not violate any of the rules. The results of this screening process are presented in **Table 1**.

**Docking and Molecular Interaction Analysis**

The amino acids present at the active site of SIRT6 protein are the following: GLU-20, LYS-31, ALA-51, GLY-52, THR-55, PHE-62, ARG-63, PRO-65, HIS-66, TRP-69, ARG-74, LYS-79, ASP-81, ARG-106, GLN-111, ASN-112, ARG-124, HIS-131 GLN-145, ARG-162, LEU-184, SER-189, LEU-190, ASP-192, ASP - 194, ARG-203, THR-213, GLN-216, SER-214, LEU-215, ILE-217 PRO-219, ASN-222, ARG-229, ARG-230, ASN-238, LEU-239, GLN-240, ARG-251, HIS-253, VAL-256, LYS-294 [55, 61]. The docking and

**Table 1. Drug-likeness screening of the 29 bioactive compounds and the two control drug.**

| S/N | Plants | Phytochemicals | Chemical Formula | Molecular weight | XLOGP | Number of H-bond acceptors | Number of H-bond donors | Bioavailability Score | Lipinski number of violations |
|---|---|---|---|---|---|---|---|---|---|
| 1 | *Buchholzia coriacea* | Oleic acid | $C_{18}H_{34}O_2$ | 282.46 | 7.64 | 2 | 1 | 0.85 | 1 |
| 2 | | Stigmasterol | $C_{29}H_{48}O$ | 412.69 | 8.56 | 1 | 1 | 0.55 | 1 |
| 3 | | Cyclooctasulphur | $S_8$ | 256.52 | 8.56 | 1 | 1 | 0.55 | 1 |
| 4 | | 5-hydroxylmethylfurfural | $C_6H_6O_3$ | 126.11 | -0.58 | 3 | 1 | 0.55 | 0 |
| 5 | | Beta-sitosterol | $C_{29}H_{50}O$ | 414.71 | 9.34 | 1 | 1 | 0.55 | 1 |
| 6 | *Vernonia amygdalina* | Vernodalin | $C_{19}H_{20}O_7$ | 360.36 | 0.31 | 7 | 1 | 0.55 | 0 |
| 7 | | Luteolin | $C_{15}H_{10}O_6$ | 286.24 | 2.53 | 6 | 4 | 0.55 | 0 |
| 8 | | Phytol | $C_{20}H_{40}O$ | 296.53 | 8.19 | 1 | 1 | 0.55 | 1 |
| 9 | | Glucurono lactone | $C_6H_8O_6$ | 176.12 | -1.85 | 6 | 3 | 0.55 | 0 |
| 10 | | Chlorogenic acid | $C_{16}H_{18}O_9$ | 354.31 | -0.42 | 9 | 6 | 0.11 | 1 |
| 11 | *Mimosa pudica* | Mimosine | $C_8H_{10}N_2O_4$ | 198.18 | -4.36 | 5 | 3 | 0.55 | 0 |
| 12 | | *p*-coumaric acid | $C_9H_8O_3$ | 164.16 | 1.46 | 3 | 2 | 0.85 | 0 |
| 13 | | Avicularin | $C_{20}H_{18}O_{11}$ | 434.35 | 0.98 | 11 | 7 | 0.17 | 2 |
| 14 | | Mimopudine | $C_{14}H_{19}N_5O_5$ | 337.33 | -2.72 | 8 | 5 | 0.55 | 0 |
| 15 | | 2-hydroxylmethyl-chroman-4-on | $C_{10}H_{10}O_3$ | 178.18 | 0.76 | 3 | 1 | 0.55 | 0 |
| 16 | *Momordica charantia* | Momordicoside k | $C_{37}H_{60}O_9$ | 648.87 | 3.67 | 9 | 5 | 0.55 | 1 |
| 17 | | Phenylalanine | $C_9H_{11}NO_2$ | 165.19 | -1.52 | 3 | 2 | 0.55 | 0 |
| 18 | | Gentisic acid 5-O-beta-glucoside | $C_{13}H_{16}O_9$ | 316.26 | -1.27 | 9 | 6 | 0.11 | 1 |
| 19 | | Quercetin-7-o-beta-d glucopyranoside | $C_{21}H_{20}O_{12}$ | 464.38 | 0.36 | 12 | 8 | 0.17 | 2 |
| 20 | | Benzoic acid | $C_7H_6O_2$ | 122.12 | 1.87 | 2 | 1 | 0.85 | 0 |
| 21 | *Bergenia ciliate* | Allantoin | $C_4H_6N_4O_3$ | 158.12 | -2.17 | 3 | 4 | 0.55 | 0 |
| 22 | | Catechin | $C_{15}H_{14}O_6$ | 290.27 | 0.36 | 6 | 5 | 0.55 | 0 |
| 23 | | Bergenin | $C_{14}H_{16}O_9$ | 328.27 | -0.97 | 9 | 5 | 0.55 | 0 |
| 24 | | Galloyl-epicatechin | $C_{22}H_{18}O_{10}$ | 442.37 | 2.3 | 10 | 8 | 0.55 | 1 |
| 25 | *Mangifera indica* | Mangiferin | $C_{19}H_{18}O_{11}$ | 422.34 | -0.37 | 11 | 8 | 0.17 | 2 |
| 26 | | Methyl gallate | $C_8H_8O_5$ | 184.15 | 0.86 | 5 | 3 | 0.55 | 0 |
| 27 | | Kaempferol | $C_{15}H_{10}O_6$ | 286.24 | 1.9 | 6 | 4 | 0.55 | 0 |
| 28 | | Protocatehuic acid | $C_7H_6O_4$ | 154.12 | 1.15 | 4 | 3 | 0.56 | 0 |
| 29 | | Luteoxanthin | $C_{40}H_{56}O_4$ | 600.87 | 9.39 | 4 | 2 | 0.17 | 2 |
| | Control Drug | Metformin | $C_4H_{11}N_5$ | 129.16 | -1.27 | 2 | 3 | 0.55 | 0 |
| | | Miglitol | $C_8H_{17}NO_5$ | 207.22 | -2.57 | 6 | 5 | 0.55 | 0 |

molecular interaction results in **Table 2** below represent the binding energies, hydrogen bonds, hydrophobic interactions, π-stackings, and salt bridges between the compounds and protein SIRT6.

The findings revealed that *Buchholzia coriacea* compounds, namely Oleic acid, Stigmasterol, Cyclooctasulphur, 5-hydroxymethylfurfural, and Beta-sitosterol, exhibited binding energy scores of -6.4 kcal/mol, -7.1 kcal/mol, -2.5 kcal/mol, -4.3 kcal/mol, and -7.0 kcal/mol, respectively. Notably, Stigmasterol displayed the highest binding affinity. In detail, Oleic acid formed six hydrogen bonds with amino acid residues ALA51, ARG63, GLY212, SER214, and LEU215, while also engaging in hydrophobic interactions with PHE62, TRP69, VAL113, HIS131, TRP186, and ILE217 **(Figure 3a)**. Stigmasterol formed two hydrogen bonds with HIS66 and LYS79 and exhibited hydrophobic interactions with THR55, ALA56, HIS66, LYS79, TYR255, and ASP257 **(Figure 3b)**. Cyclooctasulphur formed no hydrogen bonds and hydrophobic interactions with the protein target. 5-hydroxylmethylfurfural established three hydrogen

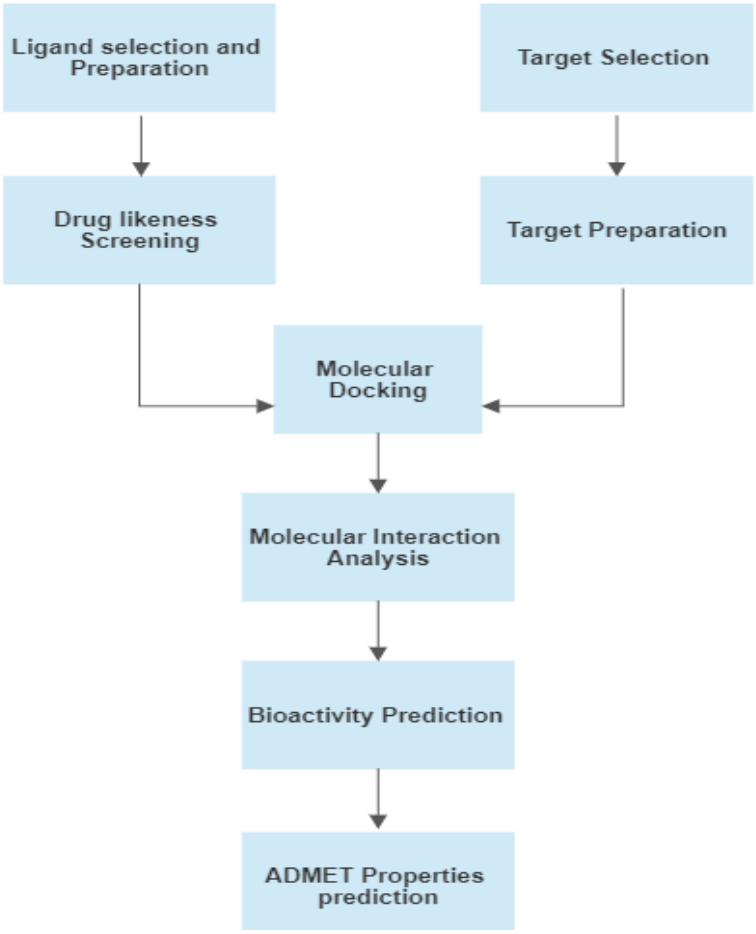


**Figure 1. Flow chart of the study.**

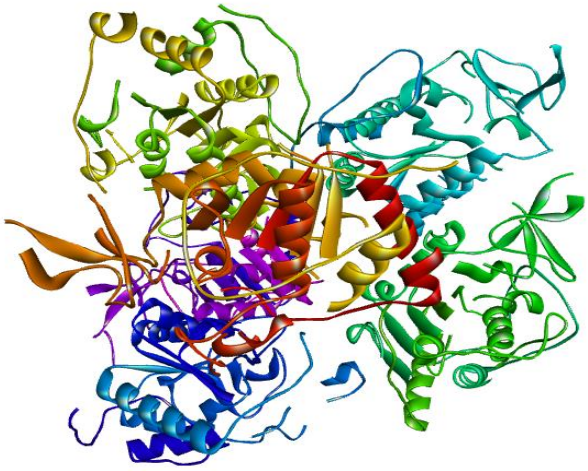

**Figure 2. Structure of the human SIRT6 (Retrieved from protein data bank).**

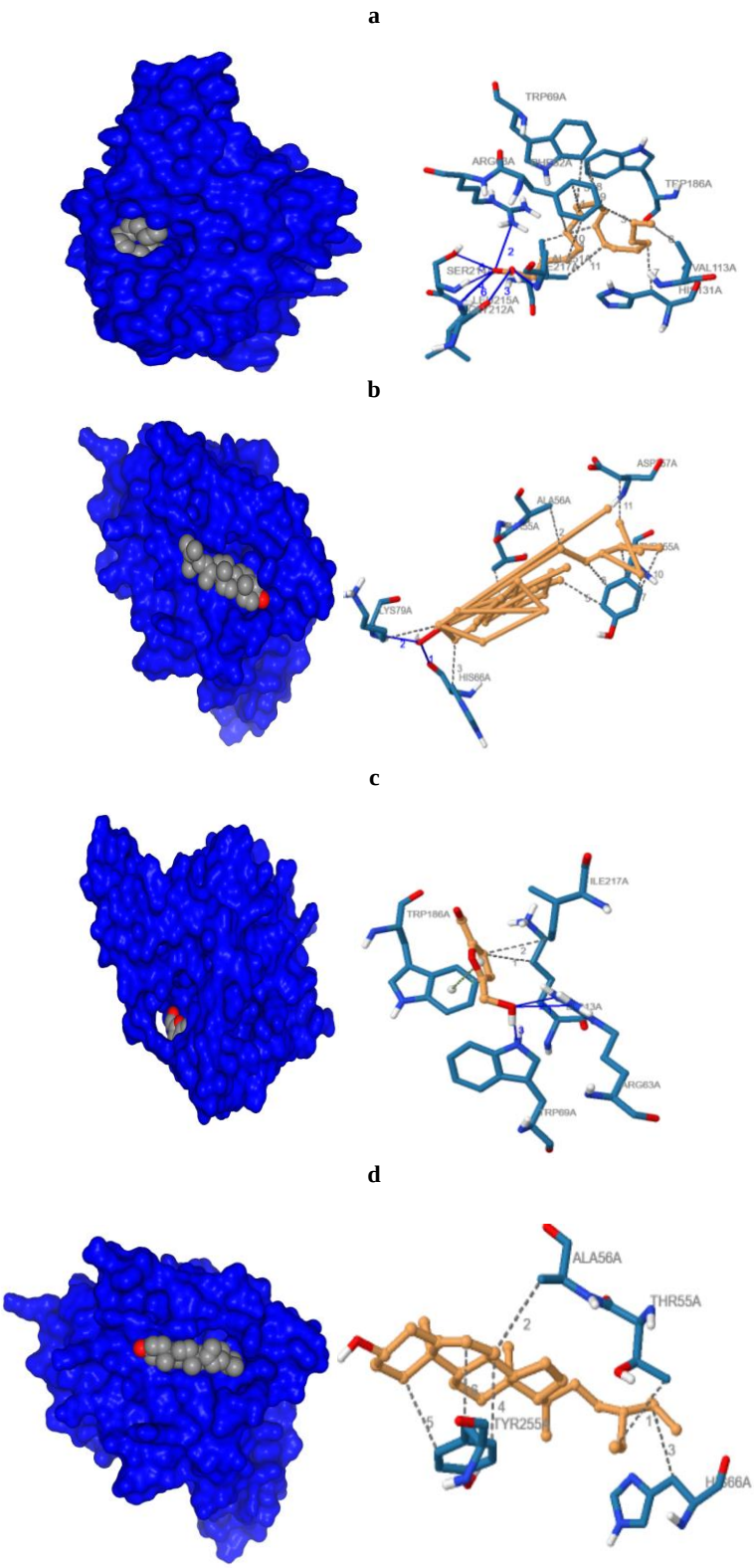


**Figure 3. The binding arrangement of Oleic acid (3a), Stigmasterol (3b), 5-hydroxymethylfurfural (3c), and Beta-sitosterol (3d) within the active site of 3K35, as determined through molecular docking using AutoDock.** Protein-Ligand Interaction Profiler and Proteins Plus online server was employed to analyze the binding interactions. The legends denote the different types of interactions: a blue dashed line represents a hydrogen bond, a green dotted line represents pi stacking, and a grey dotted line represents a hydrophobic interaction.

**Table 2. Evaluation of the molecular docking between the bioactive compounds with the target**

| S/N | Plant Source | Molecules | Binding energy (kcal/mol) | Number of hydrogen bond formed | Residues involved in hydrogen bond formation (Ă) | Residues involved in hydr0phobic interaction (Ă) | Residues involved in π-stacking (Ă) | Salt bridge |
|---|---|---|---|---|---|---|---|---|
| 1 | ***Buchholzia coriacea*** | **Oleic acid** | **-6.4** | 6 | ALA51 (2.15) ARG63 (3.50) GLY212(3.07) SER214(1.91, 2.81) LEU215(3.28) | PHE62(3.92, 3.95, 3.99, 3.70) TRP69(3.64) VAL113(3.82) HIS131(3.65) TRP186(3.87,3.74) ILE217(3.83,3.62) | | |
| | | **Stigmasterol** | **-7.1** | 2 | HIS66(2.62) LYS79(2.39) | THR55(3.60) ALA56(3.93) HIS66(3.10) LYS79(3.96) TYR255(3.54, 3.87, 3.69, 3.56, 3.93, 3.65) ASP257(3.61) | | |
| | | Cyclooctasulphur | -2.5 | NO INTERACTION | NO INTERACTION | NO INTERACTION | | |
| | | 5-hydroxylmethylfurfural | -4.3 | 3 | ARG63 (2.58, 2.39) TRP69 (2.13) | LYS13 (3.74) ILE217 (3.69) | TRP186 (4.87) | |
| | | **Beta-sitosterol** | **-7.0** | | | THR55(3.86) ALA56(3.63) HIS66(3.92) TYR255(3.56, 3.58, 3.43) | | |
| 2 | ***Vernonia amygdalina*** | Vernodalin | -5.8 | 1 | TYR255 (2.71) | THR55(3.93) PRO60(3.91) TYR255(3.89) | | |
| | | **Luteolin** | **-7.8** | 4 | HIS66(2.99) ASN238(2.40) LEU239(2.78) GLN240(2.04) | LEU239(3.65, 3.67) GLN240(3.64) | | |
| | | Phytol | -4.1 | 2 | THR83(2.35,3.41) | PHE80(3.61,3.39) VAL151(3.68) | | |
| | | Glucurono lactone | -4.9 | 3 | HIS131(3.59) TRP186(2.95,2.46) | | | LYS13 (5.40) HIS131(4.16) |
| | | **Chlorogenic acid** | **-7.7** | 6 | ASP61(2.91, 1.77) HIS66(2.99) ASP81(2.71) LEU23(2.36) VAL256(3.05) | HIS66(3.73) LEU239(3.38, 3.62) | | |
| 3 | ***Mimosa pudica*** | Mimosine | -4.3 | 5 | THR55(2.02) ASP61(2.18, 2.43) GLU64(3.18) HIS66(2.22) | | | HIS66 (5.34) |
| | | ***p*-coumaric acid** | **-6.4** | 4 | ALA51 (3.11) ARG63 (3.60) SER214 (2.30, 3.25) | PHE62(3.89) | PHE62(3.74) | |
| | | **Mimopudine** | **-7.5** | 8 | ALA51(2.94) ARG63(2.20, 2.96, 2.34) TRP69(2.85) GLN111(2.39, 2.91) HIS131(3.39) | ARG63 (3.49) VAL113 (3.70) | | |
| | | **2-hydroxy methyl-chroman-4-on** | **-5.7** | 1 | THR182 (2.09) | LEU157(3.57, 3.69) ARG180 (3.90) | | |
| 4 | ***Momordica charantia*** | **Momordicoside K** | **-6.8** | 3 | THR55(1.79) LYS79(2.90) ASP257(3.44) | THR55 (3.96) HIS66 (3.75) TYR255 (3.76) | | |

| | | | | | | | |
|---|---|---|---|---|---|---|---|
| | | **Phenylalanine** | **-5.5** | 2 | ASP185 (2.60) TRP186 (2.25) | LYS13(3.78) TRP186(3.71) ILE217((3.77, 3.87, 3.70) | HIS131 (5.19) |
| | | **Gentisic acid 5-O-beta-glucoside** | **-7.1** | 4 | HIS66(3.43) LEU239(3.10) GLN240(2.12, 2.00) | LEU239 (3.80, 3.57) | |
| | | **Benzoic acid** | **-5.7** | 5 | GLN111(3.24) SER214(2.09, 2.46) LEU215(2.42)GLN216(2.67) | ALA51(3.92) PHE62(3.89) GLN111(3.74) ILE217(3.80) | ARG63 (4.94) |
| 5 | ***Bergenia ciliate*** | **Allantoin** | **-5.3** | 6 | ARG124(3.31, 2.34) LEU127(2.53) GLN145(2.60) ASP194(2.42, 3.36) | | |
| | | **Catechin** | **-8.4** | 7 | LYS13(2.74) ALA51(2.66) ARG63(2.61, 3.19) HIS131(2.89) THR213(1.87) SER214(2.33) | LYS13(3.70 PHE62 (3,39) TRP186(3.53 ILE217(3.78, 3.71) | |
| | | **Bergenin** | **-6.8** | 6 | ARG124(2.32, 3.11, 2.75) LEU127(3.57) GLU129(3.23) GLN145 (2.52) | ARG193 (3.58) | ARG193 (4.98) |
| | | **Beta-sitosterol** | **-7.0** | | | THR55(3.86) ALA56(3.63) HIS66(3.92) TYR255(3.56,3.58, 3.43) | |
| | | **Galloyl-epicatechin** | **-7.4** | 6 | GLU20(3.07) THR55(2.55) ASP61(2.47) HIS66(3.10) LEU39(2.91) GLN240(3.62) | LEU239(3.88) TYR255(3.70) | |
| 6 | ***Mangifera indica*** | **Methyl gallate** | **-6.6** | 7 | ALA51(3.57) ARG63(3.40) GLN111(3.26) ASN112(2.35) HIS131(1.99) SER214(2.22) LEU215(3.22) | ALA51(3.59) | |
| | | **Kaempferol** | **-7.0** | 5 | ARG101(2.25, 1.70, 2.36,) GLY121(3.18) LEU287(3.31) | ARG101(3.72) LEU280(3.73,3.87, 3.68,3.78) | |
| | | **Protocatechinic acid** | **-5.3** | 1 | ALA51(2.39) | PHE62(3.43) GLN111(3.99) ILE217(3.85) | HIS131 (4.70) |
| 7 | **Control drugs** | Metformin | -4.8 | 4 | ARG124(3.32, 2.62, 2.42) GLN145(3.54) | | GLU129(4.97) ASP194(4.23, 3.74) |
| | | Miglitol | -5.1 | 5 | THR55(2.55) ASP61(2.01,1.89) HIS66(2.49,3.00) | | |

*Compounds in bold letters are the best-hit ligands*

bonds with ARG63 and TRP69 and engaged in hydrophobic interactions with LYS13 and ILE217 **(Figure 3c)**. Lastly, Beta-sitosterol solely participated in hydrophobic interactions with THR55, ALA56, HIS66, and TYR255 **(Figure 3d)**.

Our second chosen medicinal plant, *Vernonia amygdalina*, contains several bioactive compounds, including Vernodalin, Luteolin, Phytol, Glucurono lactone, and Chlorogenic acid. Vernodalin exhibited a binding score of -5.8 kcal/mol, forming a single hydrogen bond with TYR255 and engaging in hydrophobic interactions with three residues: THR55, PRO60, and TYR255 **(Figure 4a)**. Luteolin demonstrated the highest binding affinity within this plant category, binding to the protein target with an energy of -7.8 kcal/mol. As depicted in **Figure 4b**,

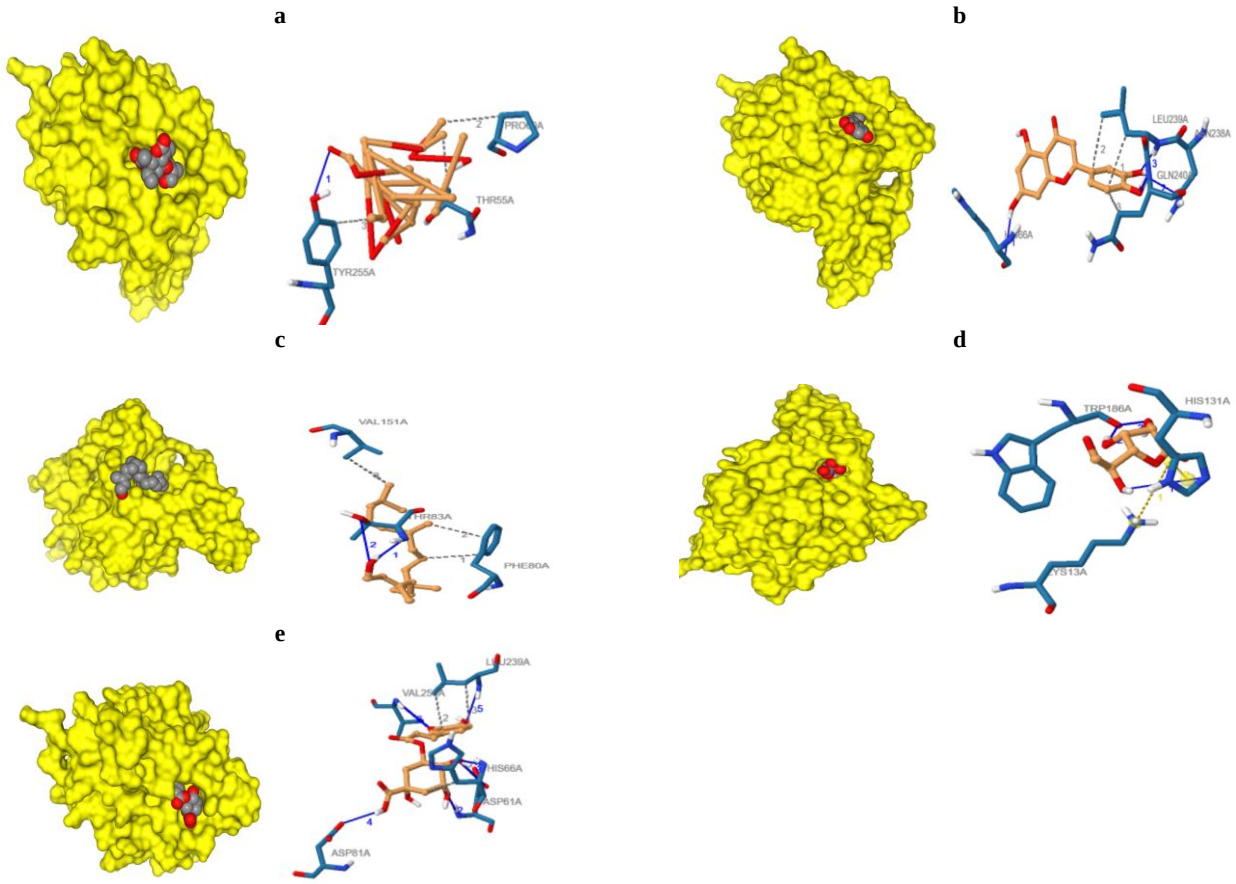


**Figure 4. The binding arrangement of Vernodalin 4(a), Luteolin 4(b), Phytol 4(c), Glucurono lactone 4(d) and Chlorogenic acid 4(e) within the active site of 3K35, as determined through molecular docking using AutoDock.** Protein-Ligand Interaction Profiler and Proteins Plus online server was employed to analyze the binding interactions. The legends denote the different types of interactions: a blue dashed line represents a hydrogen bond, a green dotted line represents pi stacking, and a grey dotted line represents a hydrophobic interaction.

Luteolin established hydrogen bonds with four amino acids: HIS66, ASN238, GLN240 and LEU239, and also exhibited hydrophobic interactions with LEU239 and GLN240. Phytol displayed a binding score of -4.1 kcal/mol, forming two hydrogen bonds with THR83 and interacting hydrophobically with PHE80 and VAL151 **(Figure 4c)**. Glucurono lactone exhibited a binding energy of -4.9 kcal/mol, establishing three hydrogen bonds with HIS131 and TRP186 and forming a salt bridge with LYS13 and HIS131 **(Figure 4d)**. Chlorogenic acid also demonstrated a favourable binding score of -7.7 kcal/mol, forming six hydrogen bonds with ASP61, HIS66, ASP81, LEU23, and VAL256 and engaging in hydrophobic interactions with HIS66 and LEU239 **(see Figure 4e)**.

Our analysis revealed that the bioactive compounds Mimosine, *p*-coumaric acid, Mimopudine, and 2-hydroxy methyl-chroman-4-on, found in *Mimosa pudica*, exhibited binding scores of -4.3 kcal/mol, -6.4 kcal/mol, -7.5 kcal/mol, and -5.7 kcal/mol, respectively, with Mimopudine demonstrating the highest binding affinity. Mimosine formed five hydrogen bonds with amino acids THR55, ASP61, GLU64, and HIS66, establishing a salt bridge with HIS66 **(Figure 5a)**. *p*-coumaric acid engaged in four hydrogen bonds with residues ALA51, ARG63, and SER214 and interacted hydrophobically with residue PHE62. Additionally, it formed a π-stacking interaction with PHE62 **(Figure 5b)**. Mimopudine established eight hydrogen bonds with residues ALA51, ARG63, TRP69, GLN111, and HIS131 and displayed hydrophobic interactions with ARG63 and VAL113 **(Figure 5c)**. Lastly, 2-hydroxy methyl-chroman-4-on formed one hydrogen bond with amino acid THR182 and interacted hydrophobically with LEU157 and ARG180 **(Figure 5d)**.

From *Momordica charantia*, we identified the bioactive compounds Momordicoside K, Phenylalanine, Gentisic acid 5-O-beta-glucoside, and Benzoic acid,

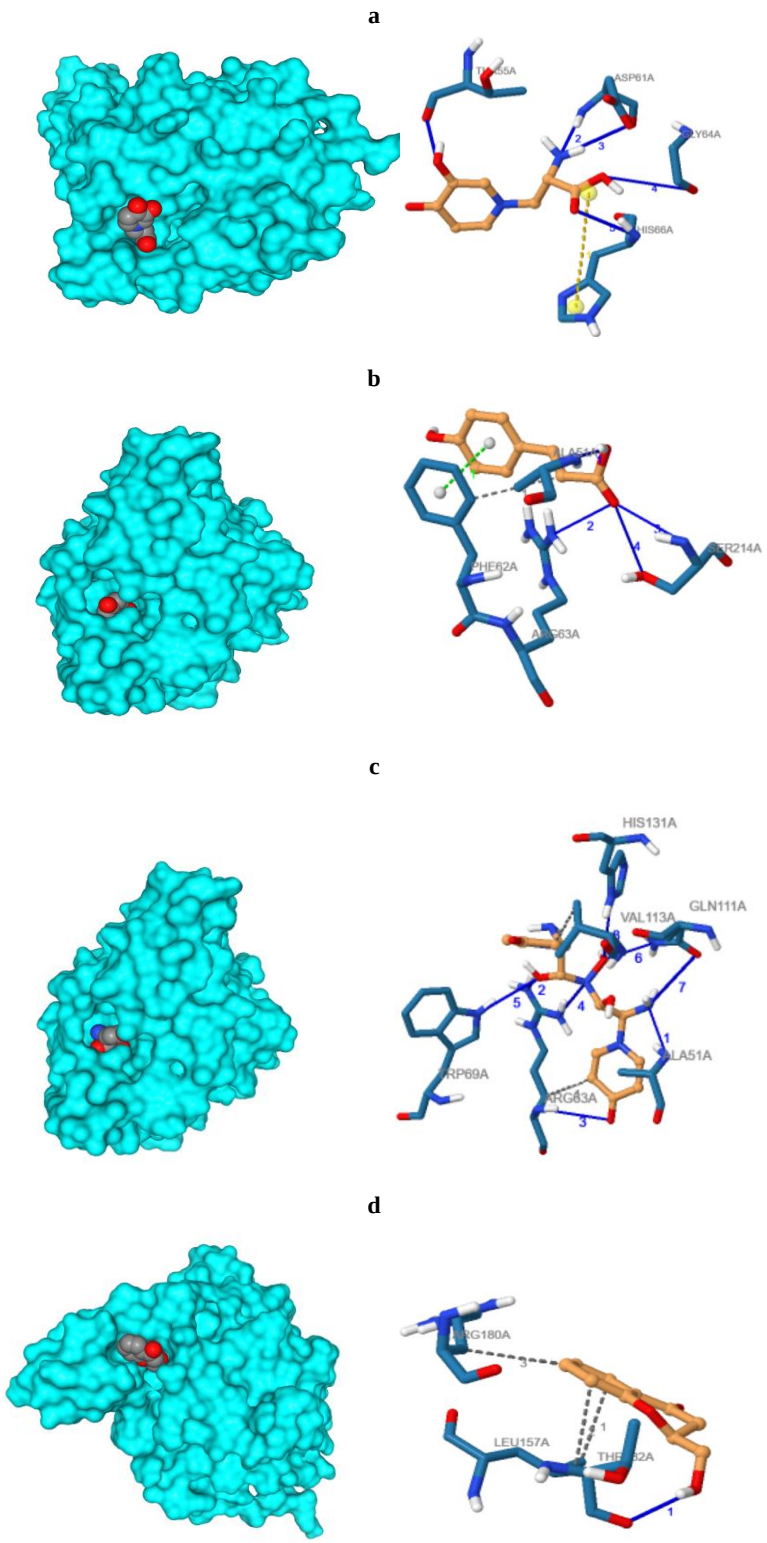


**Figure 5. The binding arrangement of Mimosine 5(a), *p*-coumaric acid 5(b), Mimopudine 5(c), and 2-hydroxy methyl-chroman-4-on 5(d) within the active site of 3K35, as determined through molecular docking using AutoDock**. Protein-Ligand Interaction Profiler and Proteins Plus online server was employed to analyze the binding interactions. The legends denote the different types of interactions: a blue dashed line represents a hydrogen bond, a green dotted line represents pi stacking, and a grey dotted line represents a hydrophobic interaction.

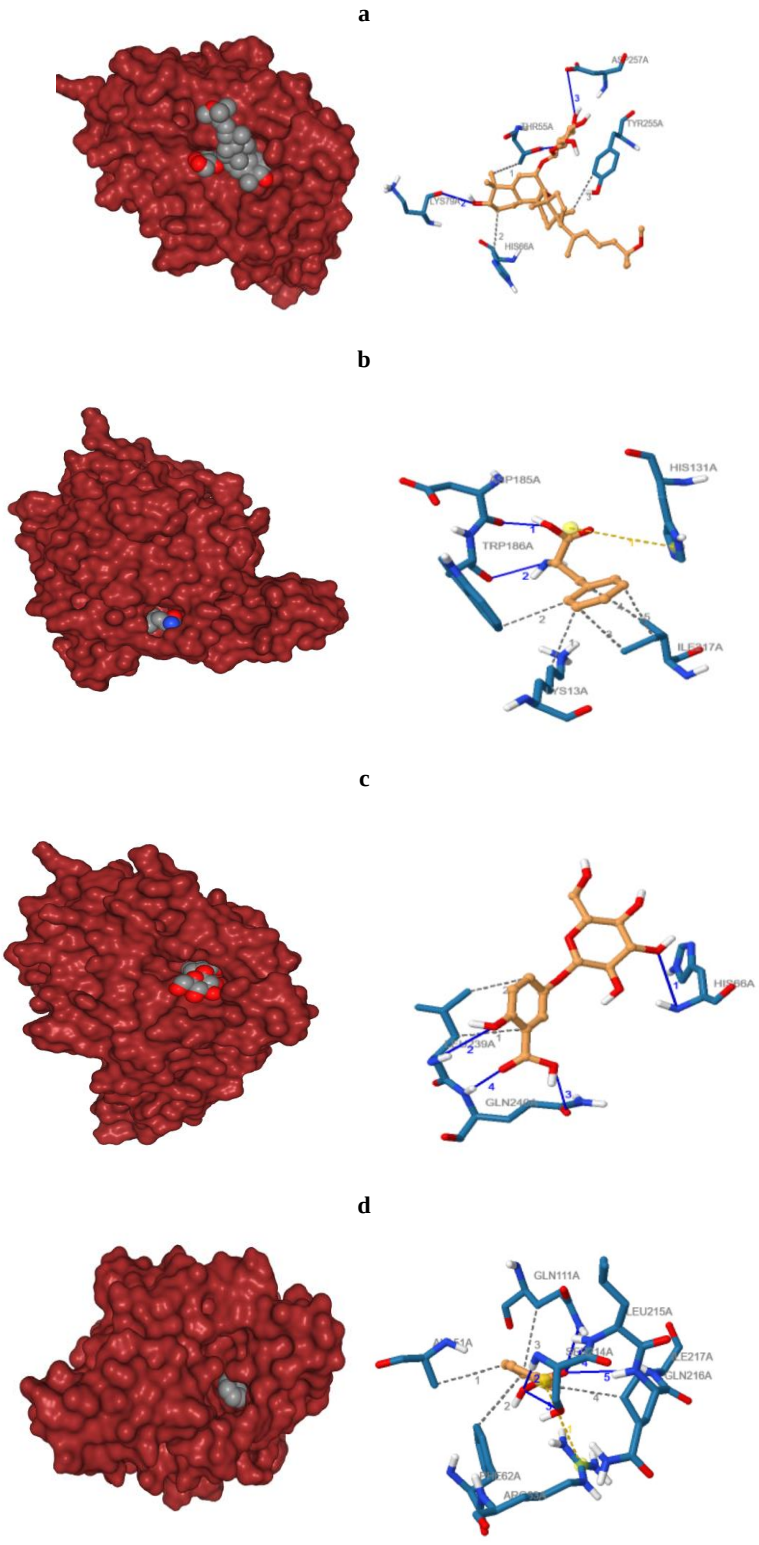


**Figure 6. The binding arrangement of Momordicoside K 6(a), Phenylalanine 6(b), Gentisic acid 5-O-beta-glucoside 6(c), and Benzoic acid 6 (d) within the active site of 3K35, as determined through molecular docking using AutoDock**. Protein-Ligand Interaction Profiler and Proteins Plus online server was employed to analyze the binding interactions. The legends denote the different types of interactions: a blue dashed line represents a hydrogen bond, a green dotted line represents pi stacking, and a grey dotted line represents a hydrophobic interaction.

which exhibited binding scores of -6.8 kcal/mol, -5.5 kcal/mol, -7.1 kcal/mol, and -5.7 kcal/mol, respectively, when interacting with the SIRT6 protein. Momordicoside K formed three hydrogen bonds with amino acids THR55, LYS79, and ASP257, and engaged in hydrophobic interactions with THR55, HIS66, and TYR255 **(Figure 6a)**. Phenylalanine established two hydrogen bonds with ASP185 and TRP186, displayed hydrophobic interactions with LYS13, TRP186, and ILE217, and formed a salt bridge with HIS131 **(Figure 6b)**. Gentisic acid 5-O-beta-glucoside established four hydrogen bonds with residues HIS66, LEU239, and GLN240 and had hydrophobic interactions with LEU239 **(Figure 6c)**. Lastly, Benzoic acid formed five hydrogen bonds with GLN111, SER214, LEU215, and GLN216, displayed hydrophobic interactions with ALA51, PHE62, GLN111, and ILE217, and formed a salt bridge with ARG63 **(Figure 6d)**.

*Bergenia ciliate* contains the following bioactive compounds, namely Allantoin, Catechin, Bergenin, Beta-sitosterol, and Galloyl-epicatechin, which exhibit binding scores of -5.3 kcal/mol, -8.4 kcal/mol, -6.8 kcal/mol, -7.0 kcal/mol, and -7.4 kcal/mol, respectively, when interacting with the protein target. Among them, Catechin shows the highest binding affinity. Allantoin forms six hydrogen bonds with amino acids ARG124, LEU127, GLN145, and ASP194 **(Figure 7a)**. Catechin establishes seven hydrogen bonds with residues LYS13, ALA51, ARG63, HIS131, THR213, and SER214, and engages in hydrophobic interactions with LYS13, PHE62, TRP186, and ILE217 **(refer to Figure 7b)**. Bergenin forms six hydrogen bonds with ARG124, LEU127, GLU129, and GLN145 and exhibits hydrophobic interactions and a salt bridge linkage with ARG193 **(Figure 7c)**. Beta-sitosterol solely interacts hydrophobically with THR55, ALA56, HIS66, and TYR255 **(refer to figure 7d).** Galloyl-epicatechin forms six hydrogen bonds with GLU20, THR55, ASP61, HIS66, LEU39, and GLN240, and engages in hydrophobic interactions with LEU239 and TYR255 **(Figure 7e)**.

*Mangifera indica* contains bioactive compounds, namely Methyl gallate, Kaempferol, and Protocatechuic acid, which exhibit binding energies of -6.6 kcal/mol, -7.0 kcal/mol, and -5.3 kcal/mol, respectively, when interacting with our target protein. Among them, Kaempferol shows the highest binding score in this category. Methyl gallate forms seven hydrogen bonds with residues ALA51, ARG63, GLN111, ASN112, HIS131, SER214, and LEU215, and interacts hydrophobically with ALA51 **(see Figure 8a)**. Kaempferol establishes five hydrogen bonds with ARG101, GLY121, and LEU287 and engages in hydrophobic interactions with residues ARG101 and LEU280 **(Figure 8b)**. Protocatechuic acid forms one hydrogen bond with residue ALA51, exhibits hydrophobic interactions with PHE62, GLN111, and ILE217, and forms a salt bridge linkage with residue HIS131 **(Figure 8c)**.

Metformin and Miglitol have a binding energy of -4.8kcal/mol and -5.1kcal/mol, respectively. Metformin forms four hydrogen bonds with amino acids ARG124 and GLN145 (3.54), and it has salt bridge linkage with residues GLU129 and ASP194 **(Figure 9a)**. Miglitol forms five hydrogen bonds with residues THR55, ASP61, and HIS66 **(Figure 9b)**.

**Bioactivity Prediction**

The bioactivity properties of the bioactive compounds with greater binding affinity than the control drugs and that of the control drugs are shown in **Table 3**.

This bioactivity includes scores for GPCR ligand, ion channel modulator, nuclear receptor legend, kinase inhibitor, protease inhibitor, and enzyme inhibitor. For the GCPR ligand, Metformin, Miglitol, Protocatechuic acid, Kaempferol, Methyl gallate, Bergenin, Benzoic acid, Allantoin, Phenylalanine, 2-hydroxymethyl chroman-4-on, Mimopudine, *p*-coumaric acid, and Luteolin has GCPR ligand score between -5.0 and 0.0 which indicates that they are moderately active. Oleic acid, Stigmasterol, Beta-sitosterol, Vernodalin, Chlorogenic acid, Momordicoside k, Gentisic acid 5-O-beta-glucoside, Galloyl-epicatechin, and Catechin has GCPR score greater than 0.0 and an indication that they are active. The ion channel modulator score of Metformin, Miglitol, Protocatechuic acid, Kaempferol, Momordicoside k, Methyl gallate, Bergenin, Benzoic acid, Allantoin, 2-hydroxy methyl chroman-4-on, *p*-coumaric acid, Luteolin, Stigmasterol, and Vernodalin ranges from -5.0 to 0.0 which indicates they are moderately active while the ion channel modulator score of Oleic acid, Beta-sitosterol, Chlorogenic acid, Galloyl-epicatechin, Catechin, Mimopudine, Phenylalanine, and Gentisic acid 5-O-beta-glucoside is greater than 0.0 which indicates they are highly active. Oleic acid, Stigmasterol, Beta-sitosterol, Vernodalin, Chlorogenic acid, Momordicoside k, Gentisic acid 5-O-beta-glucoside, Galloyl-epicatechin, *p*-coumaric acid, 2-hydroxy methyl chroman-4-on, Phenylalanine, Allantoin, Benzoic acid, Bergenin, Methyl gallate, Protocatechuic, Miglitol, and Metformin has kinase inhibitor property in between -5.0 and 0.0 which indicate that they are moderately active. Kaempferol, Luteolin, Mimopudine, and Catechin have kinase inhibitor scores greater than 0.0, indicating they are highly active. Nuclear receptor ligand is another predicted bioactivity score on the compounds of interest, Metformin, Miglitol, Protocatechuic acid, Bergenin, Benzoic acid, Phenylalanine, 2-hydroxy methyl chroman-4-on, Mimopudine, *p*-coumaric acid, Methyl gallate, and Allantoin has nuclear receptor score between -5.0 and 0.0 suggesting that they are moderately active.

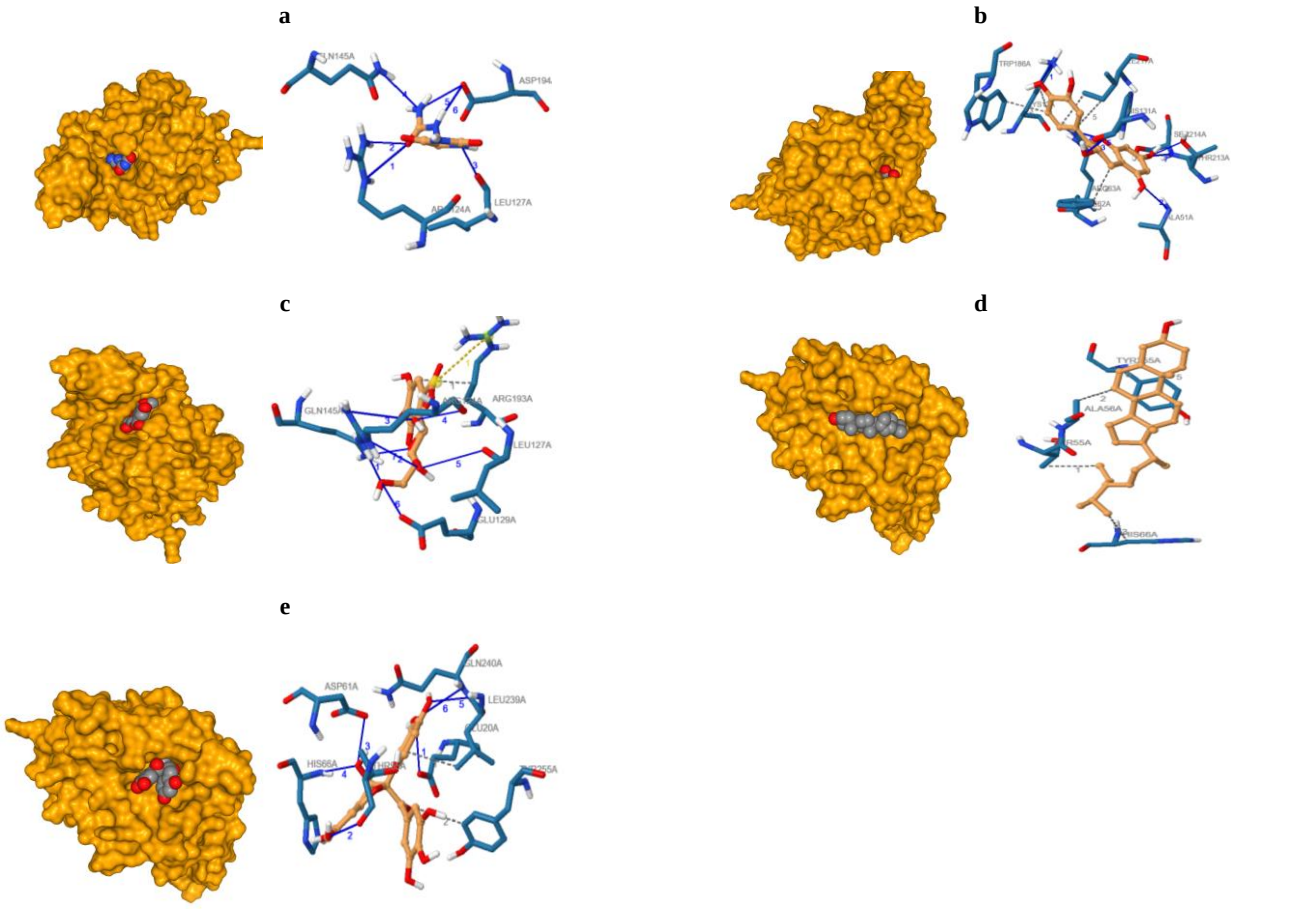


**Figure 7. The binding arrangement of Allantoin 7(a), Catechin 7(b), Bergenin 7(c), Beta-sitosterol 7(d) and Galloyl-epicatechin 7(e) within the active site of 3K35, as determined through molecular docking using AutoDock**. Protein-Ligand Interaction Profiler and Proteins Plus online server was employed to analyze the binding interactions. The legends denote the different types of interactions: a blue dashed line represents a hydrogen bond, a green dotted line represents pi stacking, and a grey dotted line represents a hydrophobic interaction.

In contrast, Oleic acid, Stigmasterol, Beta-sitosterol, Vernodalin, Luteolin, Chlorogenic acid, Momordicoside k, Gentisic acid-5-o-beta-d, Catechin, Galloyl-epicatechin, and Kaempferol has their score greater than 0.0 which suggest that they are highly active. The protease inhibitor of Stigmasterol, Luteolin, *p*-coumaric acid, 2-hydroxy methyl chroman-4-on, Phenylalanine, Allantoin, Benzoic acid, Bergenin, Methyl gallate, Kaempferol, Protocatechuic acid, and Metformin is between -5.0 and 0.0 an indication that they are moderately active. In contrast, the protease inhibitor of Oleic acid, Beta-sitosterol, Vernodalin, Chlorogenic acid, Momordicoside k, Gentisic acid-5-*O*-beta- D-glucopyranoside, Galloyl-epicatechin, Catechin, Mimopudine, and Miglitol is greater than 0.0 which indicate high activity. Enzyme inhibitor score for Allantoin, Benzoic acid, Bergenin, Methyl gallate, Protocatechuic, Metformin, 2-hydroxy methyl chroman-4-on, and *p*-coumaric acid is between -5.0 and 0.0, an indication for moderate activity while the score for Miglitol, Kaempferol, phenylalanine, Mimopudine, Luteolin, Oleic acid, Stigmasterol, Beta-sitosterol, Vernodalin, Chlorogenic acid, Momordicoside k, Gentisic acid 5-*O*-beta-glucoside, Catechin, and Galloyl-epicatechin is greater than 0.0 which indicates high activeness.

**ADMET Properties Prediction**

The absorption, distribution, metabolism, excretion, and toxicity properties of the hit compounds are shown in **Table 4** below.

For the absorption properties, Oleic acid, Stigmasterol, Beta-sitosterol, Vernodalin, Mimopudine, Phenylalanine, Benzoic acid, Allantoin, and Gentisic

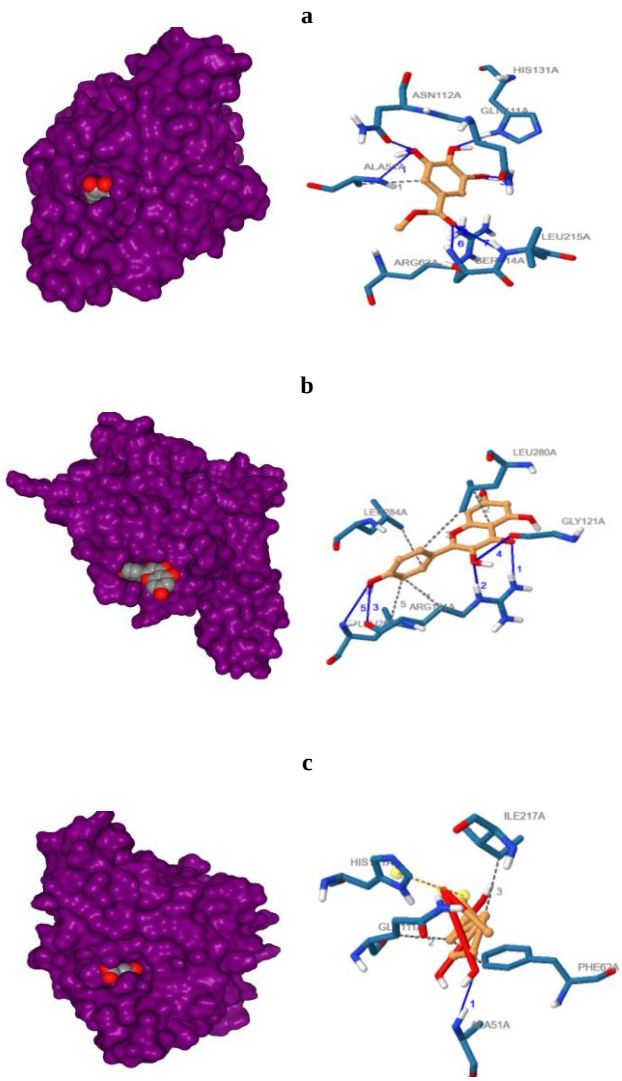


**Figure 8. The binding arrangement of Methyl gallate 8(a), Kaempferol 8(b), and Protocatechinic acid 8(c) within the active site of 3K35, as determined through molecular docking using AutoDock.** Protein-Ligand Interaction Profiler and Proteins Plus online server was employed to analyze the binding interactions. The legends denote the different types of interactions: a blue dashed line represents a hydrogen bond, a green dotted line represents pi stacking, and a grey dotted line represents a hydrophobic interaction.

acid 5-O-beta-glucoside can cross the blood-brain barrier (BBB). In contrast, Momordicoside k, Luteolin, *p*-coumaric acid, 2-hydroxy methyl chroman-4-on, Bergenin, Methyl gallate, Kaempferol, Protocatechinnic acid, Catechin, and Galloyl-epicatechin together with the two control drugs Miglitol and Metformin cannot cross the blood-brain barrier.

Oleic acid, Stigmasterol, Beta-sitosterol, Luteolin, *p*-coumaric acid, 2-hydroxy methyl chroman-4-on, Benzoic acid and Phenylalanine has high absorption in the intestine through Caco-2 permeability. In contrast, other compounds and the control drugs inclusive have low intestinal absorption. All the hit compounds except Momordicoside k are not P-glycoprotein (Pgp) inhibitors. For the distribution properties, fifteen (15) out of the twenty hit compounds and the control drugs have good plasma protein binding, which (PPB) is below 90%. Sixteen (16) out of the twenty hit compounds are predicted to be localized in the mitochondria. Metformin and Miglitol are localized in lysosomes and mitochondria, respectively. For the metabolism properties, sixteen (16) out of the twenty compounds and the control drugs were predicted not to inhibit key cytochrome P450 enzymes which are CYP450 1A2, CYP450 3A4, CYP450 2C9, CYP450 2C19, and CYP450 2D6.

**a**

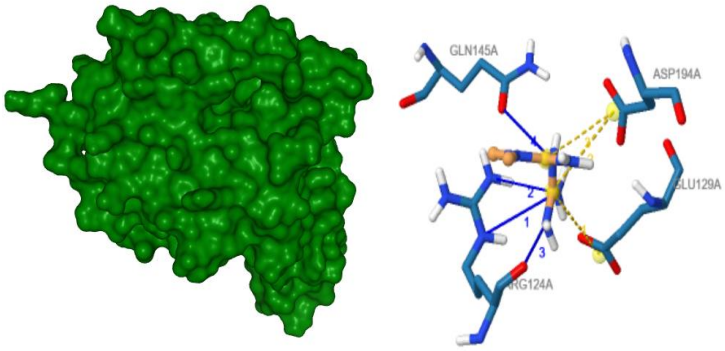


**b**

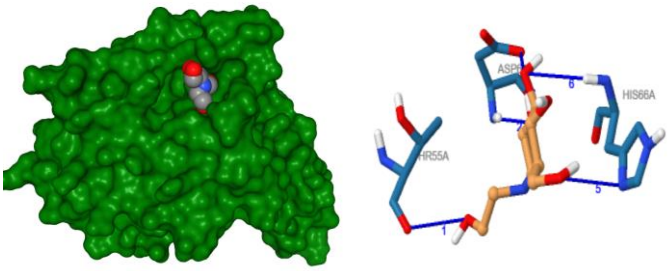


**Figure 9. The binding arrangement of Metformin 9(a) and Miglitol 9(b) within the active site 3K35, as determined through molecular docking using AutoDock.** Protein-Ligand Interaction Profiler and Proteins Plus online server was employed to analyze the binding interactions. The legends denote the different types of interactions: a blue dashed line represents a hydrogen bond, a green dotted line represents pi stacking, and a grey dotted line represents a hydrophobic interaction.

Oleic acid

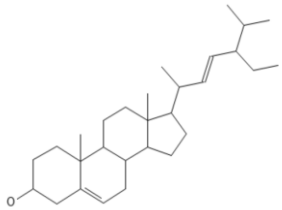

Stigmasterol

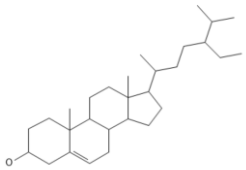

Beta-sitosterol

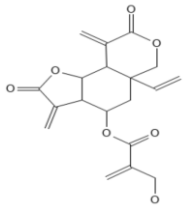

Vernodalin

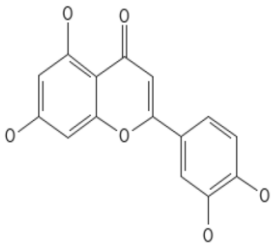

Luteolin

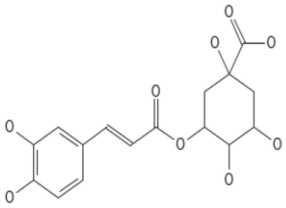

Chlorogenic acid

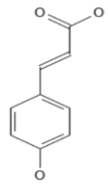

*p*-coumaric acid

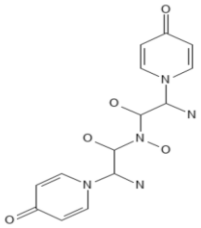

Mimopudine

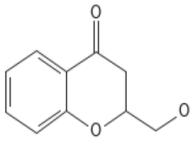

-hydroxylmethyl-chroman-4-one

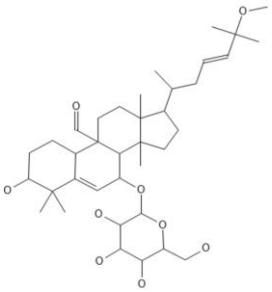

Momordicoside K

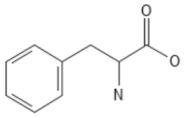

Phenylalanine

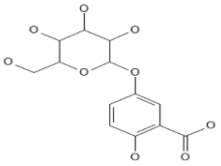

Gentisic acid 5-O-beta-glucoside

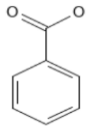

Benzoic acid

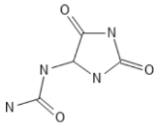

Allantoin

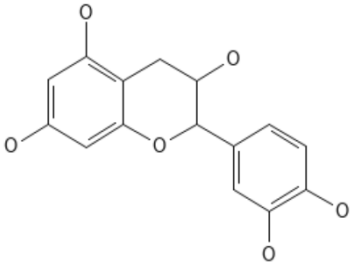

Catechin

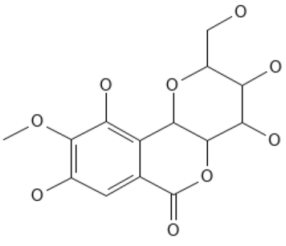

Bergenin

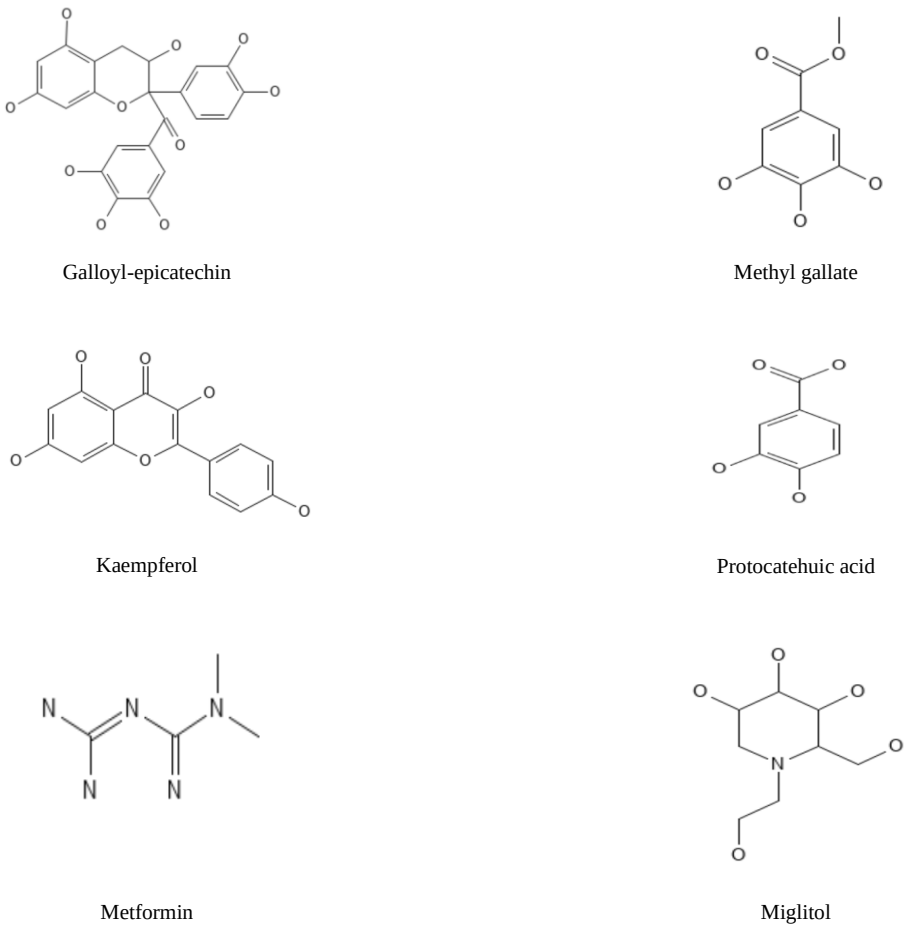


**Figure 10. 2D structure of the best-hit ligands and control drugs**

In comparison, the other four compounds could inhibit one or two enzymes. Almost all the compounds and the control drugs have good metabolic properties. For the toxicity properties, all compounds and control drugs except Stigmasterol and Momordicoside k cannot inhibit the human ether a-go-go gene, which indicates that they cannot affect the QT interval of the heart. The bioactive compounds and the control drugs, except Benzoic acid, are non-carcinogenic. Of all the bioactive compounds, Catechin, Bergenin, Galloyl-epicatechin, Kaempferol, and Luteolin are mutagenic.

## DISCUSSION

Type-2 Diabetes mellitus is a complex condition characterized by persistent high blood glucose levels and involves multiple factors. Currently, medications are available for managing the associated complications of Type-2 diabetes. However, due to their combined effects, there is a need to explore more effective and safer drugs that can effectively decrease blood glucose levels while minimizing side effects[55]. Consequently, it is crucial to identify biological targets for developing new classes of antidiabetic agents with bioactive substances and novel mechanisms. Additionally, developing molecules that can facilitate therapeutic interventions remains a primary objective. *In-silico* techniques have emerged as valuable tools for obtaining initial information about drug-likeness and understanding the mode of action, thereby saving time and resources[68]. In this study, twenty-nine (29) bioactive compounds sourced from six (6) Medicinal plants were examined through *in silico* analysis to assess their potential as antidiabetic agents. The target protein chosen for this analysis was SIRT6. The bioactive compounds were compared with the control drugs, Metformin and Miglitol. To determine their binding affinities with the SIRT6 protein, PyRx software was employed. Furthermore, online tools were utilized to predict the bioactive compounds' pharmacokinetic properties and biological activities.

**Table 3. Predicted bioactivity score for bioactive compounds and control drugs**

| S/N | Compound name | GPCR ligand | Ion channel modulator | Kinase inhibitor | Nuclear receptor ligand | Protease inhibitor | Enzyme inhibitor |
|---|---|---|---|---|---|---|---|
| 1 | Oleic acid | 0.17 | 0.07 | -0.22 | 0.23 | 0.07 | 0.27 |
| 2 | Stigmasterol | 0.12 | -0.08 | -0.48 | 0.74 | -0.02 | 0.53 |
| 3 | Beta-sitosterol | 0.41 | 0.04 | -0.51 | 0.73 | 0.07 | 0.51 |
| 4 | Vernodalin | 0.41 | -0.05 | -0.17 | 0.86 | 0.14 | 0.56 |
| 5 | Luteolin | -0.02 | -0.07 | 0.26 | 0.39 | -0.22 | 0.28 |
| 6 | Chlorogenic acid | 0.29 | 0.14 | -0.00 | 0.74 | 0.27 | 0.62 |
| 7 | *p*-coumaric acid | -0.56 | -0.26 | -0.91 | -0.12 | -0.87 | -0.15 |
| 8 | Mimopudine | -0.02 | 0.07 | 0.20 | -0.02 | 0.22 | 0.25 |
| 9 | 2-hydroxy methyl chroman-4-on | -0.45 | -0.51 | -1.11 | -0.64 | -0.98 | -0.07 |
| 10 | Momordicoside k | 0.09 | -0.69 | -0.73 | 0.05 | 0.13 | 0.28 |
| 11 | Phenylalanine | -0.22 | 0.34 | -0.89 | -0.53 | -0.09 | 0.16 |
| 12 | Gentisic acid 5-O-beta-glucoside | 0.11 | 0.02 | -0.10 | 0.19 | 0.04 | 0.43 |
| 13 | Benzoic acid | -2.21 | -1.57 | -2.49 | -2.05 | -2.31 | -1.60 |
| 14 | Allantoin | -0.87 | -0.71 | -1.35 | -1.92 | -0.92 | -0.52 |
| 15 | Catechin | 0.41 | 0.14 | 0.09 | 0.60 | 0.26 | 0.47 |
| 16 | Bergenin | -0.06 | -0.09 | -0.09 | -0.08 | -0.14 | -0.35 |
| 17 | Galloyl-epicatechin | 0.19 | 0.03 | -0.10 | 0.38 | 0.15 | 0.30 |
| 18 | Methyl gallate | -0.89 | -0.36 | -0.89 | -0.72 | -1.03 | -0.34 |
| 19 | Kaempferol | -0.10 | -0.21 | 0.21 | 0.32 | -0.27 | 0.26 |
| 20 | Protocatechinnic acid | -0.88 | -0.35 | -0.10 | -0.58 | -1.09 | -0.34 |
| 21 | Metformin | -1.61 | -0.93 | -2.38 | -3.21 | -1.39 | -1.23 |
| 22 | Miglitol | -0.41 | -0.10 | -0.53 | -0.83 | 0.11 | 0.36 |

In this study, the drug-likeness properties of the bioactive compounds and control drugs were assessed using Lipinski's rule. Lipinski's rule is a widely used guideline in drug design and development employed by pharmaceutical chemists to predict the oral bioavailability of drug molecules. According to Lipinski's rule, candidate molecules will likely exhibit good oral bioavailability if they fulfil at least three criteria[69]. These criteria include a molecular weight of ≤ 500 g/mol, an octanol-water partition coefficient (log P) of less than 5, hydrogen bond donors (OH and NH groups) of less than 5, and hydrogen bond acceptors (mainly N and O atoms) less than 10. These parameters are associated with intestinal permeability and aqueous solubility, crucial factors influencing the initial stage of oral bioavailability. In this study, 5-hydroxymethylfurfural, Vernodalin, Luteolin, Glucuro lactone, Mimosine, *p*- coumaric acid, Mimopudine, 2-hydroxy methyl-chroman-4-one, Phenylalanine, benzoic acid, Allantoin, Catechin, Bergenin, Kaempferol, Methyl gallate and Protocatechuic acid violated none of the rules. Oleic acid, Stigmasterol, Cyclooctosulphur, Beta-sitosterol, Phytol, Chlorogenic acid, Momordicoside k, Gentisic acid 5-O-beta-glucoside, and Galloyl-epicatechin violated one of the rules. Although these ligands violated one rule, they are acceptable as drug candidates due to bioavailability and non-toxicity. While Avicularin, Quercetin-7-o-beta-d-glucoropyranoside, Magniferin and Luteoxanthin violated 2 of Lipinski's rule. The control drugs Metformin and Miglitol did not violate any of the rules. The findings of this study suggest that bioactive compounds that conform to the drug-likeness criteria have the potential to be developed as oral drugs. Compounds that violate multiple rules outlined by Lipinski's rule may encounter challenges regarding bioavailability. Hence, this rule sets specific structural parameters for predicting the theoretical oral bioavailability profile and is widely employed in drug discovery endeavours. Per Lipinski's rule of five, 25 of the 29 bioactive compounds assessed in this study met the rule's criteria. This result indicates that these bioactive compounds exhibit favourable druggability and hold promise for oral drug utilization.

**Table 4. Predicted ADMET properties of bioactive compounds and control drugs**

| S/N Class | Properties | Oleic acid | Stigmasterol | Beta-sitosterol | Vernodalin | Luteolin | Chlorogenic acid | *p*-coumaric acid | Mimopudine | 2-hydroxy methyl-chroman-4-on | Momordicoside k | Phenylalanine |
|---|---|---|---|---|---|---|---|---|---|---|---|---|
| 1. Absorption | BBB | Yes | Yes | Yes | Yes | No | No | No | Yes | No | No | Yes |
| | Caco-2 permeability | Yes | Yes | Yes | No | Yes | No | Yes | No | Yes | No | Yes |
| | Pgp-inhibitor | No | No | No | No | No | No | No | No | No | Yes | No |
| | Pgp- substrate | No | Yes | Yes | No | No | No | No | No | No | Yes | No |
| 2. Distribution | PPB | 51.8% | 104.4% | 100.7% | 67% | 106.6% | 63.4% | 50.9% | 42.2% | 5.00% | 48.1% | 32.7% |
| | Sub-cellular Localization | Plasma membrane | Lysosomes | Lysosomes | Mitochondria | Mitochondria | Mitochondria | Mitochondria | Mitochondria | Mitochondria | Mitochondria | Lysosomes |
| 3. Metabolism | CYP450 1A2 inhibition | Yes | No | No | No | Yes | No | No | No | Yes | No | No |
| | CYP450 3A4 inhibition | No | No | No | No | Yes | No | No | No | No | No | No |
| | CYP450 3A4 substrate | No | Yes | Yes | Yes | No | Yes | No | No | No | Yes | No |
| | CYP450 2C9 inhibition | No | No | No | No | No | No | No | No | No | No | No |
| | CYP450 2C9 substrate | Yes | No | No | No | No | Yes | No | No | No | No | No |
| | CYP450 2C19 inhibition | No | No | No | No | No | No | No | No | Yes | No | No |
| | CYP450 2D6 inhibition | No | No | No | No | No | No | No | No | No | No | No |
| | CYP450 2D6 substrate | No | No | No | No | No | No | No | No | No | No | No |
| | UGT Catalyzed | No | Yes | Yes | Yes | Yes | No | Yes | Yes | Yes | No | No |
| 4. Toxicity | Acute oral toxicity | Class I | Class I | Class I | Class III | Class II | Class III | ClassIII | Class III | Class II | Class III | Class III |
| | hERG inhibitor | No | Yes | No | No | No | No | No | No | No | Yes | No |
| | Human hepatotoxicity | No | Yes | Yes | Yes | No | Yes | No | Yes | No | No | Yes |
| | Ames mutagenicity | No | No | No | No | Yes | No | No | No | No | No | No |
| | Carcinogens | No | No | No | No | No | No | No | No | No | No | No |

| S/N Class | Properties | Gentisic acid 5-O-beta-glucoside | Benzoic acid | Allantoin | Catechin | Bergenin | Galloyl-epicatechin | Methyl gallate | Kaempferol | Protocatechinnic acid | Metformin | Miglitol |
|---|---|---|---|---|---|---|---|---|---|---|---|---|
| 1. Absorption | BBB | Yes | Yes | Yes | No | No | No | No | No | No | No | No |
| | Caco-2 permeability | No | Yes | No | No | No | No | No | No | No | No | No |
| | Pgp-inhibitor | No | No | No | No | No | No | No | No | No | No | No |
| | Pgp- substrate | No | No | No | No | No | No | No | No | No | No | No |
| 2.Distribution | PPB | 58.1% | 54.0% | 22.5% | 101.4% | 45.4% | 89.5% | 55.1% | 109.4% | 54.6% | 7.7% | 2.0% |
| | Sub-cellular Localization | Mitochondria | Mitochondria | Mitochondria | Mitochondria | Mitochondria | Mitochondria | Mitochondria | Mitochondria | Mitochondria | Lysosomes | Mitochondria |
| 3.Metabolism | CYP450 1A2 inhibition | No | No | No | No | No | No | No | Yes | No | No | No |
| | CYP450 3A4 inhibition | No | No | No | No | No | No | No | Yes | No | No | No |
| | CYP450 3A4 substrate | No | No | No | No | Yes | Yes | No | Yes | No | No | No |
| | CYP450 2C9 inhibition | No | No | No | No | No | No | No | Yes | No | No | No |
| | CYP450 2C9 substrate | No | No | Yes | No | No | No | No | No | No | No | No |
| | CYP450 2C19 inhibition | No | No | No | No | No | No | No | Yes | No | No | No |
| | CYP450 2D6 inhibition | No | No | No | No | No | No | No | No | No | No | No |
| | CYP450 2D6 substrate | No | No | No | yes | No | Yes | No | No | No | No | Yes |
| | UGT Catalyzed | Yes | No | No | Yes | Yes | No | Yes | Yes | Yes | No | No |
| 4. Toxicity | Acute oral toxicity | Class III | Class III | Class III | Class iv | Class iii | Class iv | Class iii | Class ii | Class iii | Class iii | Class iii |
| | hERG inhibitor | No | No | No | No | No | No | No | No | No | No | No |
| | Human hepatotoxicity | No | No | Yes | No | No | Yes | Yes | Yes | Yes | Yes | No |
| | Ames mutagenicity | No | No | No | Yes | Yes | Yes | No | Yes | No | Yes | No |
| | Carcinogens | No | Yes | No | No | No | No | No | No | No | No | No |

***BB blood-brain barrier, PPB Plasma protein binding, CYP Cytochrome P450***

This study indicated that the bioactive compounds passed the drug-likeness could be used as an oral drug. Molecules that violate more than one of these rules may present bioavailability problems. This rule, therefore, establishes specific structural parameters relevant to the theoretical prediction of the oral bioavailability profile and is closely used in the creation of new drugs[70, 71]. Using Lipinski's rule of five, 25 of the 29 bioactive compounds passed this rule. This implies that these bioactive compounds have good druggability and can be used as oral drugs.

Molecular docking is employed to assess the scoring function and analyze the interactions between a protein and a ligand, enabling the prediction of the ligand molecule's binding affinity and activity. It aids in determining the optimal conformation of the ligand within the macromolecular target, such as an enzyme or receptor, to establish a stable complex. The binding free energy, a significant thermodynamic parameter, is used in this approach to assess the theoretical stability of the ligand-protein complex[72]. In this study, Among all the tested docked bioactive compounds, Catechin derived from *Bergenia ciliate* had the best binding affinity of -8.4 kcal/mol against the target compared to other ligands and the standard drugs (Table 2), Luteolin and Chlorogenic acid derived from *Vernonia amygdalin*, had a binding affinity of (-7.8 and -7.7) kcal/mol respectively, followed by Mimopudine derived from *Mimosa pudica* with a binding affinity of -7.5 kcal/mol, Galloyl epicatechin, Stigmasterol, Gentisic acid 5-O-beta-glucoside, Kaempferol, Beta-sitosterol, Bergenin, Momordicoside k, Methyl gallate, *p*-coumaric acid, Oleic acid, Vernodalin, 2-hydroxymethyl-chroman-4-one, Benzoic acid, Phenylalanine, Allantoin and Protocatechuic acid derived from the six (6) African plants had a binding affinity of (-7.4,-7.1,-7.1,-7,-7,-6.8,-6.8,-6.6,-6.4,-6.4,-5.8,-5.7,-5.7,-5.5,-5.3&-5.3) kcal/mol respectively.

Therefore, the interaction between the bioactive compounds and the human SIRT6 target can offer anti-diabetic benefits in treating type-2 diabetes by inhibiting the target protein. Additionally, the compounds demonstrate their capability to bind to the catalytic sites of the target. Among the bioactive compounds derived from the six (6) African plants, including Catechin, Luteolin, Chlorogenic acid, Mimopudine, and the remaining sixteen (16) compounds, exhibit stronger binding to human SIRT6 compared to Metformin and Miglitol, thus presenting as potent inhibitors of this receptor and potential candidates for anti-diabetic drugs. Notably, Catechin demonstrates the highest binding affinity (-8.4 kcal/mol), attributed to its chemical interactions at specific amino acid residues within the receptor's active site (Table 2). These interactions involve hydrogen bonding with LYS13, ALA51, ARG63, HIS131, THR213, and SER214, as well as hydrophobic interactions with LYS13, PHE62, TRP186, and ILE217. Luteolin exhibits binding affinity through hydrogen bonding with HIS66, ASN238, LEU239, and GLN240, as well as hydrophobic interactions with LEU239 and GLN240. Chlorogenic acid displays binding affinity through hydrogen bonding with ASP61, HIS66, ASP81, LEU239, and VAL256 and hydrophobic interactions with HIS66, LEU239, and VAL256. The above amino acid residues act as a binding pocket for the ligand. Thus, Catechin, Luteolin, Chlorogenic acid and other bioactive compounds will be more effective against human SIRT6 receptors than Metformin and Miglitol's control drugs. The interaction of these compounds with this protein may lower blood glucose levels and prevent insulin resistance, characteristic of type-2 diabetes. It may reduce the acute and chronic complications associated with diabetes mellitus. Nguyen et al.[73], in their studies, show that tannin and flavonoid family form hydrogen interaction with GLN111, THR123, and SER214, which are the three residues that seem to have a critical role in the active site of SIRT6 and hydrophobic interaction with ILE217, TRP186 and PHE62. The interaction of these residues may serve as a good prospect for treating type-2 diabetes.

The findings of this study reveal that tannins and flavonoids, including Catechin, Luteolin, Chlorogenic acid, and other bioactive compounds, exhibit similar interactions with SIRT6, thereby impeding the progression of type-2 diabetes mellitus. The inhibition of human SIRT6 by these compounds relies on their capacity to form various bonds with specific amino acid residues at the active site. Moreover, the compounds' specificity in interacting with amino acid residues at the active site of human SIRT6 prevents potential toxic effects. The binding affinities observed between the bioactive compounds (ligands) and SIRT6 in this study were stabilized through non-covalent interactions, such as hydrogen bonds, hydrophobic bonds, pi-stacking, and salt bridge formation. Rahmayanti and Fakhrurrazi have previously highlighted the significance of hydrogen bonding as an intermolecular interaction during the development of medicinal compounds, including herbal medicines. Hydrogen bonds are crucial in facilitating various cellular functions by enabling molecular interactions. In essence, hydrogen bonds are recognized as facilitators of protein-ligand binding[74].

A hydrogen bond is considered stable when its bond length is below 2.7Å. In this research, the highest binding affinity observed for Catechin can be attributed to its interaction with seven amino acid residues through hydrogen bonds, four of which have a bond length less than 2.7Å (ALA 51 (2.66), ARG 63(2.61), THR 213(1.87), and SER 214 (2.33). Furthermore, this interaction is further stabilized by hydrophobic interactions with LYS 13 (3.70), PHE 62 (3.39), TRP

186 (3.53), and ILE 217 (3.78, 3.71) at the active site of the protein. Umar et al. reported that the binding affinity is enhanced when ligands exhibit a higher ability to form hydrophobic interactions with hydrophobic amino acid residues in the binding site[75]. This finding may explain the significant binding affinity observed for this study's bioactive compounds docked against human SIRT6. Hydrophobic bonds play a crucial role in stabilizing hydrogen bonds. The results of this investigation underscore the importance of hydrogen bonding, hydrophobic bonding, pi-stacking interactions, and salt bridges in achieving a stable interaction between the ligand and the target.

Drug score values indicate the overall potential of a compound to be a drug candidate. As presented in Table 3, a Molinspiration web-based tool was used to predict the bioactivity score of the bioactive compounds against regular human receptors such as GPCRs, ion channels, kinases, nuclear receptors, proteases and enzymes. Compounds or ligands with a bioactivity score of more than 0.00 typically exhibit substantial biological activity. In contrast, values between -5.0 and 0.00 are considered moderately active molecules, and scores below -0.50 indicate that the molecules are inactive[76]. The score result of this study shows that eleven (11) bioactive compounds; Catechin, Luteolin, Chlorogenic acid, oleic acid, Stigmasterol, Vernodalin, Mimopudine, Gentisic acid 5-O-beta-glucoside, Bergenin, Galloyl epicatechin and Kaempferol have good bioactivity score (active molecules), with Catechin having the highest values for all types of drug target when compared to other test ligands while Beta-sitosterol, *p*-coumaric acid, 2-hydroxymethyl chroman- 4-one, Momordicoside k, Phenylalanine, Benzoic acid, Allantoin, Methyl gallate and the control drugs are interpreted as insufficiently active as they have low bioactivity score lesser than -5.0. For any compound to be considered a potential drug candidate in clinical trials, it should have an acceptable pharmacokinetic profile and a high safety margin with a lower probability of toxicity and potent adverse effects[77]. To evaluate the compounds' pharmaceutical, physiological, biochemical, and molecular effects, an analysis of their absorption, distribution, metabolism, excretion, and toxicity (ADMET) properties was performed using the online server ADMETlab. These properties provide insight into the pharmacological characteristics of the compounds and their ability to reach their target protein. The ADMET properties of both the control drugs and the tested ligands are presented in Table 4. The pharmacokinetic profile of the compounds, as shown in the table, reveals that only three of the hits, namely Stigmasterol, Beta-sitosterol, and Momordicoside k, act as substrates for P-glycoprotein. In contrast, the two control drugs do not exhibit such substrate activity. According to Akinwumi et al., P-glycoprotein is among the ATP-binding cassette (ABC) proteins responsible for effluxing molecules from cells, thereby preventing their bioaccumulation and eliciting a response. A compound possesses good plasma protein binding (PPB) when its predicted value is below 90%, as high protein binding may lead to a reduced therapeutic index [78]. Fifteen hit compounds, including Chlorogenic acid and Mimopudine, have PPB values below 90%, indicating a potentially higher therapeutic index.

In this study, Catechin, Chlorogenic acid, Luteolin, and Mimopudine were predicted to have no inhibitory effects on the isoforms CYP450 2C9, CYP450 2C19, and CYP450 2D6. Therefore, they are expected to be non-inhibitors of these enzymes, indicating a lower likelihood of drug-drug interactions that may lead to loss of efficacy. Furthermore, these compounds were also predicted to be non-carcinogenic, which aligns with the earlier findings from the rigorous drug-likeness screening. Carcinogenicity is a significant concern when evaluating the toxicological properties of drugs, as it can adversely affect human physiology by damaging the genome or disrupting cellular metabolic processes[79]. Catechin, Luteolin, Chlorogenic acid, Mimopudine, and other hit bioactive compounds' non-carcinogenic nature suggests their potential as viable drug candidates. However, further validation through in vitro and in vivo studies and clinical trials is necessary to confirm the inhibitory potential of these Medicinal plant-derived compounds against human SIRT6, as revealed by the molecular docking technique employed in this current work.

Our study ascertained that out of the twenty-nine (29) compounds selected from the six (6) medicinal plants *Buchholzia coriacea*, *Vernonia amygdalina*, *Mimosa pudica*, *Momordica charantia*, *Bergenia ciliate*, *and Mangifera indica only* Avicularin, Quercetin-7-o-beta-d glucopyranoside, Mangiferin, and Luteoxanthin violated two of Lipinski rule. The molecular docking process showed that twenty (20) out of the twenty-five compounds docked against the SIRT6 protein have good binding affinity than the control drugs, with Catechin, Luteolin, Chlorogenic acid, and Mimopudine having the best binding affinity within the range of -7.5 to -8.4 kcal/mol. Compared with the control drugs, this good binding affinity suggests that these compounds interact with the protein at the catalytic site and inhibit its function in diabetes pathophysiology, which may lower blood glucose levels and prevent insulin resistance. This research, however, needs further validation with molecular dynamics studies and *in-vitro* and *in-vivo* evaluation.

## CONCLUSION

Our study ascertained that out of the twenty-nine (29) compounds selected from the six (6) medicinal plants *Buchholzia coriacea*, *Vernonia amygdalina*,

*Mimosa pudica, Momordica charantia, Bergenia ciliate, and Mangifera indica only* Avicularin, Quercetin-7-o-beta-d glucopyranoside, Mangiferin, and Luteoxanthin violated two of Lipinski rule. The molecular docking process showed that twenty (20) out of the twenty-five compounds docked against the SIRT6 protein have good binding affinity than the control drugs, with Catechin, Luteolin, Chlorogenic acid, and Mimopudine having the best binding affinity within the range of -7.5 to -8.4 kcal/mol. Compared with the control drugs, this good binding affinity suggests that these compounds interact with the protein at the catalytic site and inhibit its function in diabetes pathophysiology, which may lower blood glucose levels and prevent insulin resistance. This research, however, needs further validation with molecular dynamics studies and *in-vitro* and *in-vivo* evaluation.

**Abbreviations**

DM: Diabetes mellitus
IR: Insulin resistance
ADMET: Absorption, Distribution, Metabolism, Excretion, and Toxicity
PyRx: Python prescription
BBB: Blood-brain barrier
PPB: Plasma protein binding
CYP: Cytochrome P450

**Funding Acknowledgment**

This research did not receive any specific grant from funding agencies in the public, commercial, or not-for-profit sectors.

**Conflict of interest**

The authors declare that there is no conflict of interest regarding the publication of this paper.

**Acknowledgements**

All authors acknowledge their respective institutions for providing the enabling environment to carry out this work.

## REFERENCES

1. Gupta, R.C.; Chang, D.; Nammi, S.; Bensoussan, A.; Bilinski, K.; Roufogalis, B. D. Interactions between antidiabetic drugs and herbs an overview of mechanisms of action and clinical implications. *Diabetol Metab Syndr*, **2017**, *9* (1) 59. https://doi.org/10.1186%2Fs13098-017-0254-9
2. Tiwari, A. K.; Rao, J.M. Diabetes mellitus and multiple therapeutic approaches of phytochemicals: Present status and future prospects. *Current science*, **2002**, *83* (1), 30-38.
3. Chehade, J. M.; Mooradian, A. D. A Rational Approach to Drug Therapy of Type 2 Diabetes Mellitus. *Drugs*, **2000**, *60* (1), 95–113.
4. Chen, R.; Ovbiagele, B.; Feng, W. Diabetes and Stroke: Epidemiology, Pathophysiology, Pharmaceuticals and Outcomes. *The American Journal of the Medical Sciences*, **2017**, *351* (4), 380.
5. Ogurtsova, K.; Fernandes, J. D. R.; Huang, Y.; Linnenkamp, U.; Guariguata, L.; Cho, N. H. et al. IDF Diabetes Atlas: Global estimates for the prevalence of diabetes for 2015 and 2040. *Diabetes Res Clin Pract*, **2017,** 128, 40-50. https://doi.org/10.1016/j.diabres.2017.03.024.
6. Medeiros, I.; Aguiar, A. J. F. C.; Fortunato, W. M.; Teixeira, A. F. G.; Oliveira, E.; Silva, E. G.; Bezerra, I. W. L.; Maia, J. K. D. S.; Piuvezam, G.; Morais, A. H. A. In silico structure-based design of peptides or proteins as therapeutic tools for obesity or diabetes mellitus: A protocol for systematic review and meta-analysis. *Medicine (Baltimore)*. **2023**,*102*, (15), 33514. Doi: 10.1097/MD.0000000000033514.
7. Hui, H.; Tang, G.; Go, V. L. W. Hypoglycemic herbs and their action mechanisms. *Chinese Medicine*, **2009**, 4, 11.
8. Srinivasan, K.; Viswanad, B.; Asrat, L.; Kaul, C. L.; Ramarao, P. Combination of high-fat diet-fed and low-dose streptozotocin-treated rat: a model for type 2 diabetes and pharmacological screening. *Pharmacological research*, **2005**, *52* (4), 313- 320.
9. Mostoslavsky, R.; Chua, K. F.; Lombard, D. B.; Pang, W. W.; Fischer, M. R. et al. Genomic instability and aging-like phenotype in the absence of mammalian SIRT6. *Cell*, **2006**, 315–329. https://doi.org/10.1016/j.cell.2005.11.044.
10. Derek, L.R. Current therapeutics algorithms for type 2 diabetes. *Diabetes*, **2001**, 4, 38-49.
11. Lorenzati, B.; Zucco, C.; Miglietta, S.; Lamberti, F.; Bruno, G. Oral Hypoglycemic Drugs: Pathophysiological Basis of Their Mechanism of Action. *Pharmaceuticals*, **2010**, *3* (9), 5–20.
12. Finkel, T.; Deng, C. X.; Mostoslavsky, R. Recent progress in the biology and physiology of sirtuins. *Nature*, **2009**, 587–591
13. Zhong, L.; D'Urso, A.; Toiber, D.; Sebastian, C.; Henry, R. E.; Vadysirisack, D. D. et al. The histone deacetylase Sirt6 regulates glucose homeostasis via Hif1alpha. *Cell*, **2010**, 280–293.
14. Dominy, J. E.; Lee, Y.; Jedrychowski, M, P.; Chim, H.; Jurczak, M. J. The deacetylase Sirt6 activates the acetyltransferase GCN5 and suppresses hepatic gluconeogenesis. *Mol. Cell*, **2012**, 900.
15. Dong, X.C. Sirtuin 6-A Key Regulator of Hepatic Lipid Metabolism and Liver Health. *Cell*, 2023, *12* (4), 663. doi: 10.3390/cells12040663.

16. Oteng-Mintah, S.; Asafo-Agyei, T.; Archer, M. A.; Atta-Adjei Junior, P.; Boamah, D.; Kumadoh, D. et al. Medicinal Plants for Treatment of Prevalent Diseases. *Pharmacognosy - Medicinal Plants*, **2019**.
17. Adedayo, A.; Famuti, A. In-silico studies of *Momordica charantia* extracts as potential candidates against SARS-CoV-2 targeting human main protease enzyme ($M^{pro}$). Inform Med Unlocked. **2023**, 38: 101216. doi: 10.1016/j.imu.2023.101216.
18. Anilakumar, K.; Raghavan, K.; Garlapati, P.; Ilaiyaraja, N. Nutritional, Pharmacological and Medicinal Properties of *Momordica charantia*. *International Journal of Nutrition and Food Sciences*, **2015**, *4* (1), 75–83.
19. Kumar, D. S.; Sharathnath, V. K.; Yogeswaran, P.; Harani, A.; Sudhakar, K.; Sudha, P.; Banji, D. Medicinal Potency of *Momordica charantia*. *International Journal of Pharmaceutical Sciences Review and Research*, **2010**, *1* (2), 95–100.
20. Mohammady, I.; Elattar, S.; Mohammed, S.; Madeha, E. An evaluation of antidiabetic and anti-lipidemic properties of *Momordica charantia* (bitter lemon) fruit extract in experimentally induced diabetes. *Life Science Journal*, **2012**, *9* (2), 363–374.
21. Paul, A.; Raychaudhuri, S. S. Medicinal uses and molecular identification of two *Momordica charantia* varieties –a review. *European Journal of Biology*, **2010**, *6* (2), 43–51.
22. Bhandari, M. R.; Jong-Anurakkun, N.; Hong, G.; Kawabata, J. α-Glucosidase and α-amylase inhibitory activities of Nepalese medicinal herb pakhanbhed (*Bergenia ciliata*, *Haw.*). *Food Chemistry*, **2008**, *106* (1), 247–252.
23. Khan, M.; Kumar, V. Phytopharmacological and chemical profile of *Bergenia ciliate*. *International Journal of Phytopharmacy*. **2016**, 6, 90–98.
24. Koul, B.; Kumar, A.; Yadav, D.; Jin, J. O. *Bergenia* genus: traditional uses, phytochemistry and pharmacology. *Molecules*, **2020**, *25* (23), 5555. doi:10.3390/molecules25235555.
25. Sinha, S, Evaluation of anti-tussive activity of sternb rhizome extract in mice. *Phytomedicine*, **2001**, *8* (4), 298–301.
26. Sinha, S.; Murugesan, T.; Maiti, K.; Gayen, J. R.; Pal, M.; Saha, B.P. Evaluation of anti-inflammatory potential of *Bergenia ciliata* sternb rhizome extract in rats. *Journal of Pharmacy and Pharmacology*, **2010**, *53* (2), 193–196.
27. Sinha, S.; Murugesan T.; Maiti K. et al. Antibacterial activity of *Bergenia ciliata* Rhizome. *Fitoterapia*, **2001**, *77* (2), 550–552.
28. Kakub, G.; Gulfraz, M. Cytoprotective effects of *Bergenia ciliata* stern, extract on gastric ulcer in rats. *Phytotherapy Research*, **2007**, *21* (12), 1217–1220.
29. Manandhar, N. P. A survey of medicinal plants of Jajarkot district, Nepal, *Journal of Ethnopharmacology*, **1995**, *48* (1), 1–6.
30. Oluwapelumi, E. A.; Emeka, J. I.; Johnpaul, O. O.; Emmanuel, D. D.; Miracle, E. U. et al. Ethnomedicinal uses, phytochemistry, pharmacological activities and toxicological effects of *Mimosa pudica*- A review. **2023**, 7. 1-18. https://doi.org/10.1016/j.prmcm.2023.100241.
31. Tasnuva, S. T; Qamar, U. A.; Ghafoor, K. et al. α-Glucosidase inhibitors isolated from *Mimosa pudica* L. *Natural Product Research*, **2019**, *33* (10), 1495–1499.
32. Tunna, T. S.; Ahmed, Q, U.; Uddin, A. B.; Sarker, M. Z. Weeds as alternative useful medicinal source: *Mimosa pudica* Linn. on diabetes mellitus and its complications. *Advanced Materials Research*, **2014**, (95), 49–59.
33. Muhammad, G.; Hussain, M. A.; Jantan, I.; Bukhari, S.N. A high-value medicinal plant as a source of bioactives for pharmaceuticals: *Mimosa pudica* L., a high-value medicinal plant. *Comprehensive Reviews in Food Science and Food Safety*, **2016**, *15* (2): 303–315.
34. Buchholzia Ajayi, M. G.; Lajide, L.; Amoo, I. A.; and Ayoade, W. G. Proximate, mineral and antioxidant activity of wonderful kola (Buchholzia coriacea) seed (fresh and freeze-dried). *GSC Biological and Pharmaceutical Sciences*, **2023**, *22* (02), 261–271. https://doi.org/10.30574/gscbps.2023.22.2.0074.
35. Burkill, H. M. The useful plants of West Tropical Africa. 2nd Ed. Vol. 1 Royal Botanic Gardens Kew 319.**1985**.
36. Dalziel, J. M. The Useful Plants of West Tropical Africa. Crown Agent for Oversea Government and Administrators. London 18-22. **1937**.
37. Hussen, E. M.; Endalew, S. A. In vitro antioxidant and free-radical scavenging activities of polar leaf extracts of *Vernonia amygdalina*. *BMC Complement Med Ther*. **2023**, *23* (1):146. doi: 10.1186/s12906-023-03923-y.
38. Owen, O,Y.; Amakiri A.O.; Karibi-Boteye, Y. A.Sugar lowering effect of bitter leaf (*Vernonia amygdalina*) in experimental broiler finisher chickens, Academic sciences. *Asian journal of pharmaceutical and Clinical Research*, **2011**, *4* (1), 19-21.
39. Modu, S.; Adeboye, A. E.; Maisaratu, A.; Mubi, B. M. Studies on the administration of *Vernonia amygdalina* Del. (Bitter leaf) and Glucophage on blood glucose level of alloxan induced diabetic rats. *International journal of medicinal plant and alternative medicine*, **2013**, *1* (1), 13–19.
40. Audu, S. A.; Taiwo, A. E.; Abdulraheem, R. O.; Sani, A. S; Abdulraheem, R. B.; Ilyas, M. A Study

Review of Documented Phytochemistry of *Vernonia amygdalina* (Family Asteraceae) as the Basis for Pharmacologic Activity of Plant Extract. *Journal of National Sciences Research*, **2012**, *2* (7), 1–8.

41. Akah P, Njoku O, Nwanguma A, Akunyili D (2004) Effects of aqueous leaf extract of *Vernonia amygdalina* on blood glucose and triglyceride levels on alloxan induced diabetic rats. Animal Research International, **2004**, *1* (2), 90-94.
42. Yehia, R.S.; Altwaim, S.A. An Insight into In Vitro Antioxidant, Antimicrobial, Cytotoxic, and Apoptosis Induction Potential of Mangiferin, a Bioactive Compound Derived from *Mangifera indica*. *Plants*, **2023**, *12*, 1539. https://doi.org/10.3390/plants12071539.
43. Shah, K.; Patel, M.; Patel, R.; Parmar, P. *Mangifera Indica* (Mango). *Pharmacognosy Review*, **2020**, *4* (7). https://doi.org/10.4103%2F0973-7847.65325
44. Kulkarni, V. M.; Rathod, V. K. Extraction of mangiferin from *Mangifera indica* leaves using three phase partitioning coupled with ultrasound. *Ind. Crop. Prod*, **2020**, 52, 292–297. doi: 10.1016/j.indcrop.2013.10.032.
45. Kumar, M.; Saurabh, V.; Tomar, M.; Hasan, M.; Changan, S.; Sasi M. et al. Mango (*Mangifera indica* L.) Leaves: Nutritional Composition, Phytochemical Profile, and Health-Promoting Bioactivities. *Antioxidants*, **2021**, *10* (2), 299. https://doi.org/10.3390/antiox10020299.
46. Damián-Medina, K.; Salinas-Moreno, Y.; Milenkovic, D.; Figueroa-Yáñez, L.; Marino-Marmolejo, E.; Higuera-Ciapara, I.; Vallejo-Cardona, A.; Lugo-Cervantes, E. In silico analysis of antidiabetic potential of phenolic compounds from blue corn (*Zea mays L.*) and black bean (*Phaseolus vulgaris L.*). *Heliyon*, **2020**, 6 (3), 03632. https ://doi.org/10.1016/j.heliy on.2020.e0363 2
47. Paul, A.; Raychaudhuri, S. S. Medicinal uses and molecular identification of two *Momordica charantia* varieties –a review. *European Journal of Biology*, **2010**, *6* (2), 43–51.
48. Bhandari, M. R.; Jong-Anurakkun, N.; Hong, G.; Kawabata, J. α-Glucosidase and α-amylase inhibitory activities of Nepalese medicinal herb pakhanbhed (*Bergenia ciliata*, Haw.). *Food Chemistry*, **2018**, *106* (1), 247–252.
49. Khan, M.; Kumar, V. Phytopharmacological and chemical profile of *Bergenia ciliate*. *International Journal of Phytopharmacy*, **2016**, 90–98.
50. Koul, B.; Kumar, A.; Yadav, D.; Jin, J.O. Bergenia genus: traditional uses, phytochemistry and pharmacology. *Molecules*, **2020**, *25* (23), 5555. doi: 10.3390/molecules25235555.
51. Sinha, S. Evaluation of anti-tussive activity of sternb rhizome extract in mice. *Phytomedicine*, **2001**, *8* (4), 298–301.
52. Sinha, S.; Murugesan, T.; Maiti, K.; Gayen, J. R.; Pal, M.; Saha, B.P. Evaluation of anti-inflammatory potential of *Bergenia ciliata* sternb rhizome extract in rats. *Journal of Pharmacy and Pharmacology*, **2010**, *53* (2), 193–196.
53. Sinha, S.; Murugesan, T.; Maiti, K. et al. Antibacterial activity of *Bergenia ciliata* Rhizome. *Fitoterapia*, **2001**, *72* (5), 550–552.
54. Kim, S.; Chen, J.; Cheng, T.; Gindulyte, A.; He, J.; He, S.; Li, Q.; Shoemaker, B. A.; Thiessen, P. A.; Yu, B.; Zaslavsky, L.; Zhang, J.; & Bolton, E. E; . PubChem in 2021: new data content and improved web interfaces. Nucleic Acids Res. **2019**, 49 (D1), D1388–D1395. https://doi.org/10.1093/nar/gkaa971.
55. Rao, M. M. V.; Hariprasad T. P. N. In silico analysis of a potential antidiabetic phytochemical erythrin against therapeutic targets of diabetes. *In Silico Pharmacol.* **2021**, 9, 5. https://doi.org/10.1007/s40203-020-00065-8.
56. Berman, H. M.; Westbrook, J.; Feng, Z.; Gilliland, G.; Bhat, T. N.; Weissig, H.; Shindyalov, I.N.; Bourne, P.E. The Protein Data Bank Nucleic Acids Research, **2000**, 28, 235-242.
57. Pettersen, E. F.; Goddard, T. D.; Huang, C. C.; Couch, G. S.; Greenblatt, D. M.; Meng, E.C.; Ferrin, T.E. UCSF Chimera--a visualization system for exploratory research and analysis. *J Comput Chem.* ***2021***, *25* (13):1605-12.
58. Daina, A.; Michielin, O.; Zoete, V. SwissADME: a free web tool to evaluate pharmacokinetics, drug-likeness and medicinal chemistry friendliness of small molecules. *Sci Rep*. **2017**, 7, 42717. https://doi.org/10.1038/srep42717.
59. Lipinski, C. Rule of five in 2015 and beyond: Target and ligand structural limitations, ligand chemistry structure and drug discovery project decisions. *Adv. Drug Deliv. Rev. 101*: **2016**, 34–41.
60. Trott, O.; Olson, A. J. AutoDock Vina: improving the speed and accuracy of docking with a new scoring function, efficient optimization and multithreading. *J Comput Chem*. **2010**, *31* (2):455.
61. Vo, T.H.N.; Tran, N.; Nguyen, D.; Le, L. An in silico study on antidiabetic activity of bioactive compounds in Euphorbia thymifolia Linn. SpringerPlus, **2016**, *5* (1), 1359. https://doi.org/10.1186/s4006 4-016-2631-5
62. DeLano. Scientific LLC, 400 Oyster Point Blvd., Suite 213. South San Francisco CA 940:80-1918 http://pymol.sourceforge.net. **2005**.
63. Salentin, S.; Schreiber, S.; Haupt, V.J.; Adasme, M.F.; Schroeder, M. PLIP: fully automated protein-ligand interaction profiler. *Nucleic acids research*

*43*(W1), **2015**, W443–W447. https://doi.org/10.1093/nar/gkv315.
64. Stierand, K.; Maass, P. C.; Rarey, M. Molecular complexes at a glance: automated generation of two-dimensional complex diagrams. *Bioinformatics*, **2006**, *22* (14):1710-6. DOI: https://doi.org/10.1093/bioinformatics/btl150.
65. Fricker, P. C.; Gastreich, M.; Rarey, M. Automated drawing of structural molecular formulas under constraints. *J Chem Inf. Comput Sci*, **2004**, *44* (3), 1065-78. DOI: https://doi.org/10.1021/ci049958u.
66. Khan, T.; Dixit, S.; Ahmad, R.; Raza, S.; Azad, I.; Joshi, S.; Khan, A. R. Molecular docking, PASS analysis, bioactivity score prediction, synthesis, characterization and biological activity evaluation of a functionalized 2-butanone thiosemicarbazone ligand and its complexes. *J. Chem. Biol.* **2017**, *10* (3), 91–104. https://doi.org/10.1007/s12154-017-0167-y.
67. Dong, J.; Wang, N. N.; Yao, Z. J.; Zhang, L.; Cheng, Y.; Ouyang, D.; Lu, A. P.; Cao, D. S. ADMETlab: a platform for systematic ADMET evaluation based on a comprehensively collected ADMET database. *J. Cheminform*, **2018**, *10* (1):29. https://doi.org/10.1186/s13321-018-0283-x.
68. Rathore, P. K.; Arathy, V.; Attimarad, V. S.; Kumar, P.; Roy, S. In silico analysis of gymnemagenin from Gymnemasylvestre (Retz.) R. Br. With targets related to diabetes. *J Theor Biol*, **2016**, 391, 95-101. https://doi.org/10.1016/jtbi.2015.12.004.
69. Kralj, S.; Jukič, M.; Bren, U. Molecular Filters in Medicinal Chemistry. *Encyclopedia* **2023**, *3*, 501-511. https://doi.org/10.3390/encyclopedia3020035.
70. Attique, S. A.; Hassan, M.; Usman, M.; Atif, R. M.; Mahboob, S.; Al-Ghanim, K. A.; Bilal, M., Nawaz, M. Z. A molecular docking approach to evaluate the pharmacological properties of natural and synthetic treatment candidates for use against hypertension. *International journal of environmental research and public health*, **2019**, 16, 923. doi;10.3390/ijerph16060923.
71. Nogara, P. A.; Saraiva Rde, A.; Caeran Bueno, D.; Lissner, L. J.; Lenz Dalla Corte C.; Braga, M. M.; Rosemberg, D. B.; Rocha, J. B. Virtual screening of acetylcholinesterase inhibitors using the Lipinski's rule of five and ZINC databank. Biomed Res Int. **2015**. doi: 10.1155/2015/870389.
72. McNally V. A.; Rajabi, M.; Starford, I. J.; Edwards, P. N.; Douglas, K. T.; Bryce, R. A.; Jaffar M.; Freenan S. Design, synthesis and enzymatic evaluation of 6-bridged imidazolyluracil derivatives as inhibitors of human thymidine phosphorylase. *J.Pharm.Pharmacol*., **2007**, 59, 537.
73. Nguyen, V. T. H., Tran, N., Nguyen, D.; Le, L. An in silico study on antidiabetic activity of bioactive compounds in euphorbia thymifolia Linn. *SringerPlus*, **2016**, 5, 1359. doi 10.1186/s40064-016-2631-5.
74. Rahmayanti, Y., Rizarullah, N., Fakhrurrazi, M. R. Antiviral potential of Eucalyptus oil (melaleuca cajuputi) as the primary protease inhibitor of SARS-CoV -2 revealed by molecular docking. *International journal of health science*, **2022**, *2* (2), 23-33.
75. Umar, H. I.; Josiah, S. S.; Saliu, T. P.; Jimoh T. O.; Ajayi, A.; Danjuma J. B. Insilico analysis of the inhibitor of the SARS-CoV -2 main protease by some active compounds from selected African plants. *Journal of Taibah university medical sciences*, **2021**, *16* (2), 162-176.
76. Joshi, A., Kumar, R., Sharma, A. Molecular docking studies, bioactivity score prediction, drug likeness analysis of GSK-3 inhibitors: a target protein involved in Alzheimer's disease. *Bosci: biotech res asia*, **2018**, *15* (2), 455-467.
77. Żołek, T.; Mazurek, A.; Grudzinski, I.P. In Silico Studies of Novel Vemurafenib Derivatives as BRAF Kinase Inhibitors. *Molecules*, **2023**, *28*, 5273. https://doi.org/10.3390/molecules28135273
78. Akinwumi, I. A.; Faleti, A. I.; Owojuyigbe, A. P.; Raji, F. M.; Alaka, M. M. In silico Studies of Bioactive Compounds Selected from Four African Plants with Inhibitory Activity Against Plasmodium falciparum Dihydrofolate Reductase- Thymidylate Synthase (pfDHFR-TS). *J. Adv. Pharm. Res*, **2022**, *6* (3), 107-122. DOI: 10.21608/aprh.2022.139794.1175.
79. Guo, L.; Zhen-Xing, W.; Jia-Cai, Y.; Li, F.; Zhi-Jiang Y. et al. ADMETlab 2.0: an integrated online platform for accurate and comprehensive predictions of ADMET properties. *Nucleic Acids Res*, **2021**, 49, 5 -14.